arXiv:cond-mat/0406221v1 [cond-mat.mes-hall] 9 Jun 2004

Time-Dependent Spin-Polarized Transport Through a Resonant Tunneling Structure with Multi-Terminal

Zhen-Gang Zhu, Gang Su*, Qing-Rong Zheng and Biao Jin
Department of Physics, The Graduate School of the Chinese Academy of Sciences, P. O. Box 3908, Beijing 100039, China

The spin-dependent transport of the electrons tunneling through a resonant tunneling structure with ferromagnetic multi-terminal under dc and ac fields is explored by means of the nonequilibrium Green function technique. A general formulation for the time-dependent current and the time-averaged current is established. As its application the systems with two and three terminals in noncollinear configurations of the magnetizations under dc and ac biases are investigated, respectively. The asymmetric factor of the relaxation times for the electrons with different spin in the central region is uncovered to bring about various behaviours of the TMR. The present three-terminal device is different from that discussed in literature, which is coined as a spin transistor with source. The current-amplification effect is found. In addition, the time-dependent spin transport for the two-terminal device is studied. It is found that the photonic sidebands provide new channels for the electrons tunneling through the barriers, and give rise to new resonances of the TMR, which is called as the photon-asisted spin-dependent tunneling. The asymmetric factor of the relaxation times is observed to lead to additional resonant peaks besides the photon-asisted resonances.

PACS numbers: 73.40.Gk, 73.40.Rw, 75.70.Cn

I. INTRODUCTION

Giant magnetoresistance (GMR) effect[1] discovered in Fe/Cr multilayers has motivated much research on the spin-dependent transport in hybrid magnetic multilayers in recent years[2]. Parkin et al.[3] has observed that the interlayer exchange coupling oscillates damply with the Cr or Ru spacer layer thickness in Co/Ru, Co/Cr and Fe/Cr superlattice systems, which suggests that the quantum-well states be formed in the spacer layer. This is because the electrons may meet multi-reflection at the interfaces between the ferromagnets and the spacer layer, leading to the oscillation of density of states (DOS) of electrons at the Fermi level, and thereby giving rise to the oscillation of the interlayer exchange coupling with the spacer thickness[4, 5, 6]. On the other hand, the magnetic tunnel junction (MTJ) such as the ferromagnet/insulator/ferromagnet (FM/I/FM) structure was found to display the spin-valve effect[7]. The MTJ with double tunnel barriers such as FM/I/FM/I/FM structure was shown to reveal more interesting behaviors on the variation of the tunnel magnetoresistance (TMR) with bias[8]. Recently, advances in nanolithography and thin-film processing make it possible to fabricate very small double tunnel junctions called the single electron transistor (SET). With a very narrow spacer, the Coulomb interaction is important and may lead to new phenomena such as Coulomb blockade. Further investigation about the spin-dependent transport in a ferromagnetic SET[9] was performed intensively in the sequential tunneling regime[10][11] and in the cotunneling regime[12, 13]. In the former case, the oscillation of the TMR with a dc bias is observed; while the TMR in the latter case is enhanced in the strong tunneling regime, and the Coulomb blockade region is squeezed by the spin accumulation caused by the cotunneling. It would be interesting to consider another limit where the size of the spacer is not so small that the Coulomb interaction is weak, and the quantum well states can be formed in the spacer. If an ac field is applied to the leads and the central spacer, one would expect that the interesting features of the TMR might appear due to new effective tunneling channels from the photonic sidebands[14] induced by the ac field.

On the other hand, Johnson[15] demonstrated that the multi-terminal system is as important as the two-terminal system. In the so-called spin dipolar switching device (i.e. the FM/nonmagnetic metal(NM)/FM structure), the current flows from one FM layer and out of the NM layer, while the other FM layer referenced to the NM layer serves as a voltmeter to give an output voltage which depends on the magnetization configuration of the two ferromagnets[15]. Fert and Lee[16] interpreted Johnson's experiment by means of the Boltzmann equation, and at almost the same time, Hershfield et al.[17] proposed a set of weak coupling equations to describe Johnson's experiment. By invoking the framework of the scattering matrix theory (SMT) developed by Landauer and Büttiker[18] for the mesoscopic devices with multi-terminal, Brataas et al.[19, 20] discussed a three-terminal device which is to some extent different from Johnson's experimental layout, where the current does not flow out of the NM layer but out of another FM layer, and the NM layer serves as a central spacer region, while a third FM layer is introduced to measure the chemical potential and no net current flows through it. In other words, the current entering the third FM lead is equal to that flowing out of it. It is found that the direction of the magnetization of the third FM lead can affect remarkably the current flowing through the first and the second FM leads when the magnetizations of these two leads align antiparallel. In this case,

the intrinsic spin relaxation time in the central spacer was assumed to be sufficiently shorter than the order of the time between successive tunneling events such that the spin accumulation effect[21] could be negligible. Furthermore, Jedema *et al.*[22, 23] investigated the spin injection and spin accumulation in an all-metal lateral mesoscopic spin valve with multi-terminal. All these works were performed under dc biases. As mentioned before, if an ac electric field is applied to the magnetic hybrid junction with multi-terminal, one would expect that different spin-dependent transport behaviors of the electrons might appear.

In this paper, the time-dependent spin-polarized transport of a resonant tunneling structure with ferromagnetic multi-terminal will be investigated by means of the nonequilibrium Green function technique (NEGFT). It is presumed that every terminal and the central spacer are applied by the ac fields. In our model, although the spin accumulation could present, as we shall pay our attention to the current and TMR in response to ac fields, the spin accumulation will not be considered, which will be given elsewhere. A general current formalism for such a system with N terminals which are made of ferromagnetic materials or normal metals in the presence of an ac electrical field will be developed. A three-terminal device, to be coined as a spin transistor with source (STS), in which every terminal is applied by a source bias, and there is net current flowing through each of them, will be proposed. The amplification effect of the electrical curent by changing the direction of the magnetization of the third FM terminal in a STS will be discussed. The photon-assisted spin-dependent tunneling in a two-terminal device under an ac bias voltage will be explored.

The rest of this paper is organized as follows. In Sec. II, a model is proposed and a general formalism for the time-dependent current in a resonant tunneling system with ferromagnetic multi-terminal is derived. In Sec. III, the systems with two and three terminals in dc steady states are discussed. In Sec. IV, the spin-dependent transport under an ac bias for a system with two ferromagnetic terminals in which the magnetic moments are noncollinearly aligned is investigated. In Sec. V, a brief summary will be presented.

II. MODEL HAMILTONIAN AND GENERAL FORMULATION

A. Hamiltonian and the Uncoupled Green Function

Consider a resonant tunneling structure with ferromagnetic multi-terminal (RTSFMT) with the Hamiltonian given by

$$H = H_{leads} + H_{center} + H_{coupling}, \tag{1}$$

where $H_{leads} = \sum_\alpha H_\alpha$ ($\alpha = 1, 2, 3, ...$) is the Hamiltonian of the ferromagnetic leads with H_α the Hamiltonian of the αth lead, $H_{center} = \sum_\sigma \varepsilon_d(t) d_\sigma^\dagger d_\sigma$ is the Hamiltonian of the central spacer with $\varepsilon_d(t) = \varepsilon_0 + \Delta_d(t)$ the single-particle energy in the central spacer modulated by a time-varying external field where ε_0 is the single-particle level in the absence of the external field, $\Delta_d(t)$ is the energy from the time-varying field applied to the central region, and $d_\sigma^\dagger(d_\sigma)$ is the creation (annihilation) operator of an electron with spin σ in the central region. Here we presume that the single-particle energy level, say $\varepsilon_d(t)$, which can be viewed as a single-impurity level or a single energy level of quantum well states[24, 25, 26], is spin-degenerate. This case corresponds to a nonmagnetic island where the numbers of electrons with spin up $N_{d\uparrow}$ and down $N_{d\downarrow}$ are equal. In the equilibrium (e.g. in the absence of an external bias), the net moment at the nonmagnetic island is zero, while in the nonequilibrium (e.g. in the presense of an external field) the numbers of electrons with spin up and down have different tunneling rates entering into the island, and also have different tunneling rates escaping from the island. Thus, if the spin relaxation time is not very short (for example, longer than the tunneling time), the spin accumulation will occur. In the present model, we shall pay attention to the spin-dependent transport of the current and the TMR of the structure, and we will not discuss the effect of spin accumulation here for clarity[27]. $H_{coupling}$ is the coupling interaction between the leads and the central region, defined by

$$H_{coupling} = \sum_\alpha H_{T\alpha}, \tag{2}$$

$$H_{T\alpha} = \sum_{k_\alpha \sigma\sigma'} [T_{k_\alpha d}^{\sigma\sigma'}(t) \gamma_{k_\alpha \sigma}^\dagger d_{\sigma'} + h.c.], \tag{3}$$

where $\gamma_{k_\alpha\sigma}^\dagger$ is the creation operator of an electron in the αth lead with momentum k_α and spin σ, $T_{k_\alpha d}^{\sigma\sigma'}(t)$ is the element of the tunneling matrix which describes the coupling between the leads and the central region, and depends

on time, spin and momentum. We assume that all leads are ferromagnetic, and one of them is chosen as the lead 1. The magnetization of the lead 1 is presumed to align along the z axis, and the magnetizations of the other leads are supposed to deviate the z axis by angles θ_2, θ_3, $\cdots$, etc. The Hamiltonian of the lead 1 can be written as

$$H_1 = \sum_{k\sigma} \varepsilon^1_{k\sigma}(t) a^\dagger_{k\sigma} a_{k\sigma}, \tag{4}$$

where $a^\dagger_{k\sigma}(a_{k\sigma})$ is the creation (annihilation) operator of an electron of the lead 1 with momentum k and spin σ, $\varepsilon^1_{k\sigma}(t) = \varepsilon_k(t) - \sigma M_1$ is the single-particle energy modulated by a time-dependent external field with $\varepsilon_k(t) = \varepsilon_k(0) + \Delta_1(t)$, $\sigma = \pm 1$, $M_1 = \frac{1}{2} g\mu_B h_1$ with g the Landé factor, μ_B the Bohr magneton, and h_1 the molecular field of the lead 1. For the noncollinear configuration of the magnetic moments of the leads, the Hamiltonians of the other leads read

$$H_b = \sum_{k_b\sigma} \{[\varepsilon_{k_b}(t) - \sigma M_b \cos\theta_b] \widetilde{b}^\dagger_{k_b\sigma} \widetilde{b}_{k_b\sigma} - M_b \sin\theta_b \widetilde{b}^\dagger_{k_b\sigma} \widetilde{b}_{k_b\overline{\sigma}}\}, \tag{5}$$

where $b = 2, 3, \cdots$ denotes the lead 2, 3, $\cdots$, etc., k_b is the electron momentum in the lead b, $\widetilde{b}^\dagger_{k_b\sigma}(\widetilde{b}_{k_b\sigma})$ is the creation (annihilation) operator of an electron in the lead b with spin σ ($\overline{\sigma} = -\sigma$), $\varepsilon_{k_b}(t) = \varepsilon_{k_b}(0) + \Delta_b(t)$ with $\Delta_b(t)$ the energy from the time-dependent external field applied to the lead b, and $M_b = \frac{1}{2} g\mu_B h_b$ with h_b the molecular-field of the lead b. In terms of Eq.(3), we have the coupling Hamiltonian between the lead b (= 2, 3...) and the central region

$$H_{Tb} = \sum_{k_b\sigma\sigma'} [T^{\sigma\sigma'}_{k_b d}(t) \widetilde{b}^\dagger_{k_b\sigma} d_{\sigma'} + h.c.]. \tag{6}$$

By performing the $u - v$ transformation

$$\begin{aligned} \widetilde{b}_{k_b\sigma} &= \cos\frac{\theta_b}{2} b_{k_b\sigma} - \sigma \sin\frac{\theta_b}{2} b_{k_b\overline{\sigma}}, \\ \widetilde{b}^\dagger_{k_b\sigma} &= \cos\frac{\theta_b}{2} b^\dagger_{k_b\sigma} - \sigma \sin\frac{\theta_b}{2} b^\dagger_{k_b\overline{\sigma}}, \end{aligned}$$

to H_b, we find that H_b becomes

$$H_b = \sum_{k_b\sigma} \varepsilon^b_{k_b\sigma}(t) b^\dagger_{k_b\sigma} b_{k_b\sigma}, \tag{7}$$

with $\varepsilon^b_{k_b\sigma}(t) = \varepsilon_{k_b}(0) - \sigma M_b + \Delta_b(t)$. Consequently, the coupling Hamiltonian becomes

$$H_{Tb} = \sum_{k_b\sigma\sigma'} [T^{\sigma\sigma'}_{k_b d}(t)(\cos\frac{\theta_b}{2} b^\dagger_{k_b\sigma} d_{\sigma'} - \sigma \sin\frac{\theta_b}{2} b^\dagger_{k_b\overline{\sigma}} d_{\sigma'}) + h.c.]. \tag{8}$$

To this end, the Hamiltonian of the system is well defined. In a time-dependent case, the current conservation can be expressed as

$$\sum_\alpha j^c_\alpha(t) - e\frac{dN_d(t)}{dt} = 0, \ \alpha = 1, 2, 3...$$

where $j^c_\alpha(t)$ is the tunneling current flowing from the αth lead to the central spacer, while $j^d(t) = edN_d(t)/dt$ is the displacement current, with $N_d(t) = \sum_\sigma \langle d^\dagger_\sigma d_\sigma \rangle$ being the occupation number of electrons with the energy level $\varepsilon_d(t)$ in the central spacer. Recently, there are a few works towards partitioning the displacement current into each terminal[28, 29]. Likewise, the displacement current in the present case is supposed to be partitioned into every terminal in such a way, i.e. $J^d(t) = \sum_\alpha J^d_\alpha(t)$, that we have $\sum_\alpha [J^c_\alpha(t) + J^d_\alpha(t)] = \sum_\alpha J_\alpha(t) = 0$, where $J_\alpha(t) = J^c_\alpha(t) + J^d_\alpha(t)$ is the total current flowing from the αth lead into the central scattering region, and $J^c_\alpha(t) = -\frac{ie}{\hbar} \langle [H, N_\alpha] \rangle = -\frac{ie}{\hbar} \langle [H_{T\alpha}, N_\alpha] \rangle$ with N_α the particle occupation number operator in the αth lead. By means of the nonequilibrium Green function technique[30, 31], after some calculations, we obtain

$$J^c_\alpha(t) = \frac{2e}{\hbar} \Re e \sum_{k_\alpha} Tr_\sigma [\mathbf{Q}^\alpha_{k_\alpha d}(t_1) \mathbf{G}^<_{k_\alpha d}(t_1, t)],$$

where

$$\mathbf{Q}^{\alpha}_{k_\alpha d}(t_1) = \mathbf{R}_\alpha \mathbf{T}_{k_\alpha d}(t_1),$$

$$\mathbf{R}_\alpha = \begin{pmatrix} \cos\frac{\theta_\alpha}{2} & \sin\frac{\theta_\alpha}{2} \\ -\sin\frac{\theta_\alpha}{2} & \cos\frac{\theta_\alpha}{2} \end{pmatrix},$$

$$\mathbf{T}_{k_\alpha d} = \begin{pmatrix} T^{\uparrow\uparrow}_{k_\alpha d} & T^{\uparrow\downarrow}_{k_\alpha d} \\ T^{\downarrow\uparrow}_{k_\alpha d} & T^{\downarrow\downarrow}_{k_\alpha d} \end{pmatrix},$$

$\mathbf{G}^{<}_{k_\alpha d}(t,t') = \begin{pmatrix} G^{\uparrow\uparrow,<}_{k_\alpha d}(t,t') & G^{\downarrow\uparrow,<}_{k_\alpha d}(t,t') \\ G^{\uparrow\downarrow,<}_{k_\alpha d}(t,t') & G^{\downarrow\downarrow,<}_{k_\alpha d}(t,t') \end{pmatrix}$ is the lesser function in spin space with $G^{\sigma\sigma',<}_{k_\alpha d}(t,t') = i\left\langle c^{\dagger}_{k_\alpha\sigma}(t') d_{\sigma'}(t)\right\rangle$, and θ_α is the angle between the magnetization direction of the αth lead and the z axis. By using the equation of motion of the Green function, and then noting the Langreth theorem[31], we get

$$J^c_\alpha(t) = \frac{2e}{\hbar}\Re e \sum_{k_\alpha}\int dt_1 Tr_\sigma[\mathbf{G}^r_d(t,t_1)\mathbf{\Sigma}^<_\alpha(t_1,t) + \mathbf{G}^<_d(t,t_1)\mathbf{\Sigma}^a_\alpha(t_1,t)], \tag{9}$$

where $\mathbf{G}^<_d(t,t') = \begin{pmatrix} \mathbf{G}^{\uparrow\uparrow<}_d(t,t') & \mathbf{G}^{\downarrow\uparrow<}_d(t,t') \\ \mathbf{G}^{\uparrow\downarrow<}_d(t,t') & \mathbf{G}^{\downarrow\downarrow<}_d(t,t') \end{pmatrix}$ is the lesser function of the central spacer in spin space, with $\mathbf{G}^r_d(t,t')$ being the retarded Green function of the central spacer in spin space:

$$\mathbf{G}^r_d(t,t_1) = \begin{pmatrix} G^{\uparrow\uparrow,r}_d(t,t_1) & G^{\uparrow\downarrow,r}_d(t,t_1) \\ G^{\downarrow\uparrow,r}_d(t,t_1) & G^{\downarrow\downarrow,r}_d(t,t_1) \end{pmatrix},$$

where $G^{\sigma\sigma',r}_d(t,t') = -i\left\langle T\left\{d_\sigma(t)\, d^{\dagger}_{\sigma'}(t')\right\}\right\rangle$. In Eq.(9), $\mathbf{\Sigma}^\gamma_\alpha(t_1,t_2)$ ($\gamma = <, >, r, a$) is corresponding to the lesser, greater, retarded and advanced self-energy, respectively, which is defined as

$$\mathbf{\Sigma}^\gamma_\alpha(t_1,t_2) = \sum_{k_\alpha}(\mathbf{Q}^\alpha_{k_\alpha d}(t_1))^{\dagger}\mathbf{g}^\gamma_{k_\alpha}(t_1,t_2)(\mathbf{Q}^\alpha_{k_\alpha d}(t_2)),\ \gamma = <, >, r, a, \tag{10}$$

where $\mathbf{g}^\gamma_{k_\alpha}(t_1,t_2)$ is the corresponding Green functions of uncoupled leads, with the retarded (advanced) Green function given by

$$\mathbf{g}^{r(a)}_{k_\alpha}(t,t') = \mathbf{g}^{r(a)}_{k_\alpha\sigma}(t-t')\exp(\mp i\int_{t'}^{t} dt''\Delta_\alpha(t'')),$$

and the lesser function of the uncoupled leads given by

$$\begin{aligned}\mathbf{g}^<_{k_\alpha}(t,t') \;=\; & i\begin{pmatrix} f(\varepsilon^\alpha_{k_\alpha\uparrow})\exp(\mp i\varepsilon^\alpha_{k_\alpha\uparrow}(t-t')) & 0 \\ 0 & f(\varepsilon^\alpha_{k_\alpha\downarrow})\exp(\mp i\varepsilon^\alpha_{k_\alpha\downarrow}(t-t')) \end{pmatrix} \\ & \cdot\exp(\mp i\int_{t'}^{t} dt''\Delta_\alpha(t'')),\end{aligned}$$

where f is the Fermi function. When the central region is uncoupled to the leads, the retarded Green function of the central region can be obtained exactly:

$$g^r_d(t,t') = -i\theta(t-t')\exp\left\{-i\int_{t'}^{t} dt''\left[\varepsilon_0 + \Delta_d(t'')\right]\right\}.$$

B. Self-Energy Σ and the Line-Width Function Γ

From Eq.(10), we shall calculate the self-energy. The off-diagonal elements of the coupling matrix describe the spin-flip scattering processes, which was discussed in Ref.[32]. To focus on the low-temperature properties of the transport, where the available electrons near the Fermi level are dominant in the transport process, it is reasonable to ignore the effect of the spin-flip scattering during the tunneling process, and the coupling parameters are presumed to be independent of momentum. Therefore, we have $\mathbf{T}_{k_\alpha d} = \begin{pmatrix} T_{\alpha\uparrow} & 0 \\ 0 & T_{\alpha\downarrow} \end{pmatrix}$. To perform the momentum summation of the electrons, we may first sum the momenta of electrons in the uncoupled Green functions of leads. Then, for the retarded and the advanced Green functions of the uncoupled leads, we will obtain the real part Λ and the imaginary part Γ. Because Λ makes the energy levels shifted and can be absorbed into the energy level of the central spacer, we only consider the imaginary part Γ. With this consideration, one may get

$$\mathbf{\Sigma}^r_\alpha(t,t') = -\frac{i}{2}\int \frac{d\varepsilon}{2\pi} e^{-i\varepsilon(t-t')}\mathbf{\Gamma}_\alpha(\theta_\alpha,\varepsilon,t,t')e^{-i\int_{t'}^{t} dt''\Delta_\alpha(t'')}, \tag{11}$$

where the line-width function $\mathbf{\Gamma}_\alpha$ is

$$\mathbf{\Gamma}_\alpha(\theta_\alpha,\varepsilon,t,t') = \begin{pmatrix} \Gamma^\alpha_{\uparrow\uparrow}(\theta_\alpha,\varepsilon,t,t') & \Gamma^\alpha_{\uparrow\downarrow}(\theta_\alpha,\varepsilon,t,t') \\ \Gamma^\alpha_{\downarrow\uparrow}(\theta_\alpha,\varepsilon,t,t') & \Gamma^\alpha_{\downarrow\downarrow}(\theta_\alpha,\varepsilon,t,t') \end{pmatrix}, \tag{12}$$

with

$$\Gamma^\alpha_{\uparrow\uparrow}(\theta_\alpha,\varepsilon,t,t') = 2\pi\sum_{k_\alpha} T^*_{\alpha\uparrow}(t)T_{\alpha\uparrow}(t')\left[\cos^2\frac{\theta_\alpha}{2}\delta(\varepsilon-\varepsilon^\alpha_{k_\alpha\uparrow}) + \sin^2\frac{\theta_\alpha}{2}\delta(\varepsilon-\varepsilon^\alpha_{k_\alpha\downarrow})\right],$$

$$\Gamma^\alpha_{\downarrow\downarrow}(\theta_\alpha,\varepsilon,t,t') = 2\pi\sum_{k_\alpha} T^*_{\alpha\downarrow}(t)T_{\alpha\downarrow}(t')\left[\sin^2\frac{\theta_\alpha}{2}\delta(\varepsilon-\varepsilon^\alpha_{k_\alpha\uparrow}) + \cos^2\frac{\theta_\alpha}{2}\delta(\varepsilon-\varepsilon^\alpha_{k_\alpha\downarrow})\right],$$

$$\Gamma^\alpha_{\uparrow\downarrow}(\theta_\alpha,\varepsilon,t,t') = 2\pi\sum_{k_\alpha} \sin\frac{\theta_\alpha}{2}\cos\frac{\theta_\alpha}{2}T^*_{\alpha\uparrow}(t)T_{\alpha\downarrow}(t')\left[\delta(\varepsilon-\varepsilon^\alpha_{k_\alpha\uparrow}) + \delta(\varepsilon-\varepsilon^\alpha_{k_\alpha\downarrow})\right],$$

$$\Gamma^\alpha_{\downarrow\uparrow}(\theta_\alpha,\varepsilon,t,t') = 2\pi\sum_{k_\alpha} \sin\frac{\theta_\alpha}{2}\cos\frac{\theta_\alpha}{2}T^*_{\alpha\downarrow}(t)T_{\alpha\uparrow}(t')\left[\delta(\varepsilon-\varepsilon^\alpha_{k_\alpha\uparrow}) + \delta(\varepsilon-\varepsilon^\alpha_{k_\alpha\downarrow})\right].$$

Then, the lesser self-energy is

$$\mathbf{\Sigma}^<_\alpha(t,t') = i\int \frac{d\varepsilon}{2\pi} e^{-i\varepsilon(t-t')}f_\alpha(\varepsilon)\mathbf{\Gamma}_\alpha(\theta_\alpha,\varepsilon,t,t')e^{-i\int_{t'}^{t} dt''\Delta_\alpha(t'')}, \tag{13}$$

where $f_\alpha(\varepsilon)$ is the Fermi function of the αth lead. As a result, the current can be expressed as

$$\begin{aligned} J^c_\alpha(t) \;=\; & -\frac{e}{\hbar}\Im m\int dt'\int\frac{d\varepsilon}{2\pi}e^{-i\varepsilon(t'-t)}e^{-i\int_t^{t'} dt''\Delta_\alpha(t'')}Tr_\sigma \\ & \left\{\mathbf{\Gamma}_\alpha(\theta_\alpha,\varepsilon,t',t)\left[\mathbf{G}^<_d(t,t') + 2f_\alpha(\varepsilon)\mathbf{G}^r_d(t,t')\right]\right\}. \end{aligned} \tag{14}$$

It is nothing but the current flowing out of the αth terminal.

C. Equation of Motion of the Green Functions

Let us first specify the forms of the energy shifts caused by application of ac biases to the leads and the central spacer. They bear the usual forms:

$$\Delta_\alpha(t) = V_\alpha \cos(\omega_\alpha t), \tag{15}$$

$$\Delta_d(t) = V_0 \cos(\omega_0 t), \tag{16}$$

where $\omega_{\alpha(0)}$ is the frequency of the corresponding external ac bias to the αth lead (the central spacer), and $e = \hbar = 1$ is assumed.

By applying the nonequilibrium Green function technique, we get the equation of motion of the retarded Green function

$$(i\partial_t - \varepsilon_d(t))\mathbf{G}_d^r(t,t') = \delta(t-t')\mathbf{I} + \int dt_1 \mathbf{\Sigma}^r(t,t_1)\mathbf{G}_d^r(t_1,t'), \tag{17}$$

where $\mathbf{\Sigma}^r(t,t_1) = \sum_\alpha \mathbf{\Sigma}_\alpha^r(t,t_1)$ with $\mathbf{\Sigma}_\alpha^r$ being defined above. Performing the gauge transformation[33]

$$\mathbf{G}_d^r(t,t') = \widetilde{\mathbf{G}}_d^r(t,t') \exp(-i\int_{t'}^{t} dt'' V_0 \cos(\omega_0 t'')), \tag{18}$$

and introducing the double-time Fourier transform

$$F(\omega,\omega') = \int dt dt' F(t,t') \exp[i(\omega t - \omega' t')],$$

$$F(t,t') = \int \frac{d\omega}{2\pi}\frac{d\omega'}{2\pi} F(\omega,\omega') \exp[-i(\omega t - \omega' t')],$$

Eq.(17) is transformed into

$$(\omega - \varepsilon_0)\widetilde{\mathbf{G}}_d^r(\omega,\omega') = 2\pi\delta(\omega-\omega') + \int \frac{d\omega''}{2\pi}\widetilde{\mathbf{\Sigma}}^r(\omega,\omega'')\widetilde{\mathbf{G}}_d^r(\omega'',\omega'). \tag{19}$$

$\widetilde{\mathbf{\Sigma}}^r(\omega,\omega'')$ can be gained by applying the same gauge transformation and the double-time Fourier transform to $\mathbf{\Sigma}^r(t,t')$. Then substituting it into Eq.(19), we can in principle get the Green function $\widetilde{\mathbf{G}}_d^r(\omega,\omega')$. To simplify the treatment, we will assume without loss of generality that the elements of the tunneling matrix are independent of time and $\mathbf{\Gamma}_\alpha$ is taken at the Fermi energy[33]. By changing the summation into an integral, we obtain

$$[\omega - \varepsilon_0 + \frac{i}{2}\mathbf{\Gamma}(0)]\widetilde{\mathbf{G}}_d^r(\omega,\omega') = 2\pi\delta(\omega-\omega'), \tag{20}$$

where $\mathbf{\Gamma}(0) = \sum_\alpha \mathbf{\Gamma}_\alpha(0)$ with

$$\mathbf{\Gamma}_\alpha(0) = \begin{pmatrix} \Gamma_\uparrow^\alpha(0)(1+P_\alpha\cos\theta_\alpha) & \Gamma_{\uparrow\downarrow}^\alpha(0)P_\alpha\sin\theta_\alpha \\ \Gamma_{\downarrow\uparrow}^\alpha(0)P_\alpha\sin\theta_\alpha & \Gamma_\downarrow^\alpha(0)(1-P_\alpha\cos\theta_\alpha) \end{pmatrix}, \tag{21}$$

with $\Gamma_\uparrow^\alpha(0) = 2\pi\rho_\alpha^0 |T_{\alpha\uparrow}|^2$, $\Gamma_\downarrow^\alpha(0) = 2\pi\rho_\alpha^0 |T_{\alpha\downarrow}|^2$, $\Gamma_{\uparrow\downarrow}^\alpha(0) = 2\pi\rho_\alpha^0 T_{\alpha\uparrow}^* T_{\alpha\downarrow}$, $\Gamma_{\downarrow\uparrow}^\alpha(0) = 2\pi\rho_\alpha^0 T_{\alpha\downarrow}^* T_{\alpha\uparrow}$ and $\rho_\alpha^0 = \rho_{\alpha\uparrow} + \rho_{\alpha\downarrow}$, where $\rho_{\alpha\uparrow}(\rho_{\alpha\downarrow})$ is the DOS of spin up (down) subband of the αth ferromagnetic lead, while $P_\alpha = (\rho_{\alpha\uparrow} - \rho_{\alpha\downarrow})/(\rho_{\alpha\uparrow} + \rho_{\alpha\downarrow})$ is the polarization of the αth lead. So the retarded Green function of the central region becomes

$$\widetilde{\mathbf{G}}_d^r(\omega,\omega') = 2\pi[\omega - \varepsilon_0 + \frac{i}{2}\mathbf{\Gamma}(0)]^{-1}\delta(\omega-\omega'), \tag{22}$$

where the superscript -1 means the inverse of the matrix. By tranforming $\widetilde{\mathbf{G}}_d^r(\omega,\omega')$ back, one gets

$$\mathbf{G}_d^r(t,t') = \int \frac{d\omega}{2\pi} e^{-i\omega(t-t')} e^{-i\int_{t'}^{t} dt'' V_0 \cos(\omega_0 t'')} [\omega - \varepsilon_0 - \frac{i}{2}\mathbf{\Gamma}(\mathbf{0})]^{-1}. \tag{23}$$

$\mathbf{G}_d^<(t,t')$ can be obtained by the Keldysh equation

$$\mathbf{G}_d^<(t,t') = \int dt_1 dt_2 \mathbf{G}_d^r(t,t_1)\mathbf{\Sigma}^<(t_1,t_2)\mathbf{G}_d^a(t_2,t'), \tag{24}$$

where $\mathbf{\Sigma}^<(t_1,t_2) = \sum_\alpha \mathbf{\Sigma}_\alpha^<(t_1,t_2)$. With the presumption of $\mathbf{\Gamma}$ being real, we obtain the current of the αth terminal under an ac external bias:

$$\begin{aligned} J_\alpha^c(t) \;=\; & -\frac{e}{\hbar}\int \frac{d\omega}{2\pi} Tr_\sigma\{2f_\alpha(\omega)\Im m[\mathbf{\Gamma}_\alpha(0)\mathbf{A}_\alpha(\omega,t)] \\ & +\Re e\ \mathbf{\Gamma}_\alpha(0)\sum_\beta f_\beta(\omega)\mathbf{A}_\beta(\omega,t)\mathbf{\Gamma}_\beta(0)\mathbf{A}_\beta^\dagger(\omega,t)\}, \end{aligned} \tag{25}$$

where the function $\mathbf{A}_\alpha$ of the αth lead is defined as

$$\mathbf{A}_\alpha(\omega,t) = \int_{-\infty}^{t} dt' e^{i\omega(t-t')} e^{i\int_{t'}^{t} dt'' V_\alpha \cos(\omega_\alpha t'')} \mathbf{G}_d^r(t,t'). \tag{26}$$

The displacement current, $J^d(t) = edN_d(t)/dt = ed[Tr_\sigma \Im m \mathbf{G}_d^<(t,t)]/dt$, can be obtained by

$$J^d(t) = \sum_\alpha J_\alpha^d(t) \tag{27}$$

with

$$J_\alpha^d(t) = -e\Re e \frac{d}{dt}\int \frac{d\omega}{2\pi} f_\alpha(\omega) Tr_\sigma \left[\mathbf{A}_\alpha(\omega,t)\mathbf{\Gamma}_\alpha(0)\mathbf{A}_\alpha^\dagger(\omega,t)\right]. \tag{28}$$

The current conservation now becomes $\sum_\alpha [J_\alpha^c(t) + J_\alpha^d(t)] = \sum_\alpha J_\alpha(t) = 0$, where $J_\alpha(t) = J_\alpha^c(t) + J_\alpha^d(t)$ is the total current of the αth lead. Eqs. (25) and (28) are the main results of this paper. Based on them, we can investigate the spin-dependent transport in a hybrid junction system with multi-terminal under either a dc bias or an ac bias. In the following, we shall discuss the case in a steady state under a dc bias, and then, we shall consider the spin-dependent transport in a system with two and three ferromagnetic terminals whose magnetizations are noncollinearly aligned under dc and ac biases.

III. STEADY STATE UNDER A DC BIAS

A. Two Ferromagnetic Terminals with Noncollinear Configuration of Magnetizations

Let us consider the structure whose schematic layout is shown in Fig. 1. We assume that the molecular field of the left FM lead is aligned along the z axis which is perpendicular to the current direction, while the magnetization direction of the right FM lead deviates the z axis by an angle θ. A dc bias is applied between the left and the right ferromagnets, which causes a difference of chemical potential of the left and the right lead by $\mu_L - \mu_R = eV$. In a steady state, there should be no charge accumulation in the central scattering region. So the displacement current is zero, and $J_L^c = -J_R^c$ holds. For the convenience of calculation, we then define the current flowing through the system as

$$J = \frac{1}{2}(J_L^c - J_R^c). \tag{29}$$

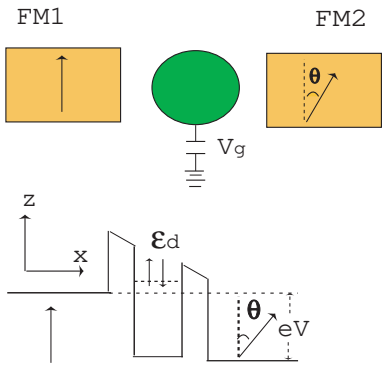


FIG. 1: (Color online) The schematic layout of a resonant tunneling system with two ferromagnetic terminals. The energy level of the central spacer can be modulated by tuning the gate voltage. The potential profile is shown in the lower panel. The magnetizations between the left and the right ferromagnetic leads deviate by an angle θ.

According to Eq.(25), we need to calculate the function $\mathbf{A}_\alpha(\varepsilon, t)$. In the steady state, we have

$$\mathbf{A}_\alpha(\varepsilon, t) = -\int \frac{d\omega'}{2\pi} \frac{i\mathbf{G}_d^r(\omega')}{\omega' - \varepsilon - i0^+}, \tag{30}$$

where $\tau = t - t'$. In addition, we have

$$\mathbf{G}_d^r(\omega) = [\omega - \varepsilon_0 + \frac{i}{2}\mathbf{\Gamma}(\mathbf{0})]^{-1}, \tag{31}$$

where $\mathbf{\Gamma} = \mathbf{\Gamma}_L + \mathbf{\Gamma}_R$. By noting that the pole of $\mathbf{G}_d^r(\omega)$ is on the lower half-plane, while the pole of the integral function of $\mathbf{A}_\alpha(\varepsilon, t)$ is on the upper half-plane ($\omega' = \varepsilon + i0^+$), one can make use of the residual theorem and perform a contour integral on the upper half-plane, and obtain the function $\mathbf{A}_\alpha(\varepsilon)$ in a steady state:

$$\mathbf{A}_\alpha(\varepsilon) = \mathbf{G}_d^r(\varepsilon). \tag{32}$$

It is obvious that the function $\mathbf{A}$ is the Fourier transform of the retarded Green function in a steady state. From Eq.(29), we arrive at

$$J = \frac{2e}{h}\int d\omega [f_L(\omega) - f_R(\omega)] T_{eff}(\omega), \tag{33}$$

where $T_{eff}(\omega) = \frac{1}{4} Tr_\sigma[\mathbf{\Gamma}_L \mathbf{G}_d^r(\omega)\mathbf{\Gamma}_R \mathbf{G}_d^a(\omega) + \mathbf{\Gamma}_R \mathbf{G}_d^r(\omega)\mathbf{\Gamma}_L \mathbf{G}_d^a(\omega)]$ is the effective transmission coefficient (ETC), and from Eq.(12), $\mathbf{\Gamma}_{L,R}$ have forms of

$$\mathbf{\Gamma}_L = \begin{pmatrix} \Gamma_\uparrow^L(0)(1+P_L) & 0 \\ 0 & \Gamma_\downarrow^L(0)(1-P_L) \end{pmatrix},$$

$$\mathbf{\Gamma}_R = \begin{pmatrix} \Gamma_\uparrow^R(0)(1+P_R\cos\theta) & \Gamma_{\uparrow\downarrow}^R(0) P_R \sin\theta \\ \Gamma_{\downarrow\uparrow}^R(0) P_R \sin\theta & \Gamma_\downarrow^R(0)(1-P_R\cos\theta) \end{pmatrix},$$

with $\Gamma_{\uparrow\downarrow}^R(0) = \Gamma_{\downarrow\uparrow}^R(0)$ (Recall that $\mathbf{\Gamma}$ is supposed to be real).

Before making the numerical calculation, it is better to specify the parameters. First, we assume that the tunnel junction under interest is symmetric, say, the two FM terminals are made of the same ferromagnets. Then, we may take $P_L = P_R = P$, and $\Gamma_{\uparrow(\downarrow)}^L(0) = \Gamma_{\uparrow(\downarrow)}^R(0) = \Gamma_{\uparrow(\downarrow)}$, $\Gamma_{\uparrow\downarrow}^R(0) = \Gamma_{\uparrow\downarrow}$. Defining a parameter which is called as the spin asymmetry factor $\eta = \Gamma_\uparrow/\Gamma_\downarrow$, which is similar but different to that in Ref.[11], we may write $\Gamma_\uparrow/\Gamma = \eta/(1+\eta)$,

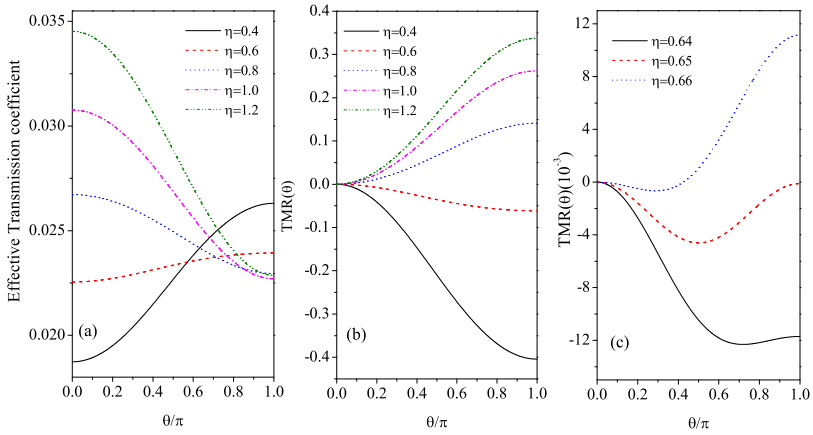


FIG. 2: (Color online) The angle θ dependence of the ETC (a) and the $TMR(\theta)$ (b) and (c) for different η. The energy is scaled by Γ, and the parameters are set as $P = 0.4$, $\varepsilon_0 = 5$, and $E_f = 8$.

$\Gamma_\downarrow/\Gamma = 1/(1+\eta)$, $(\Gamma_{\uparrow\downarrow}/\Gamma)^2 = \eta/(1+\eta)^2$ with $\Gamma = \Gamma_\uparrow + \Gamma_\downarrow$ as an energy scale hereafter. At low temperature and a small bias, the tunnel conductance C can be obtained from Eq.(33): $C = \frac{2e^2}{h} T_{eff}(E_f)$ with E_f the Fermi energy. The tunnel magnetoresistance $TMR(\theta)$ can be defined as $TMR(\theta) = 1 - C(\theta)/C_P$, where $C_P = C(\theta = 0)$ is the tunnel conductance when the magnetizations of the two FM leads are aligned parallel.

The θ dependences of the ETC and $TMR(\theta)$ for different η are presented in Figs. 2(a) and (b). It is seen that the ETC ($TMR(\theta)$) increases (decreases) with increasing θ when $\eta \lesssim 0.6$, while it decreases (increases) with increasing θ when $\eta > 0.7$. $TMR(\theta)$ becomes negative when η is small. The tunnel conductance and the TMR are remarkably affected by the spin asymmetry factor η which is the ratio of $\Gamma_\uparrow$ and $\Gamma_\downarrow$, while $\Gamma_\uparrow$ ($\Gamma_\downarrow$) is the tunneling rate of electrons with spin up (down) from the left or right electrode to the energy level in the central island. Different η means different tunneling rate for up- and down-spin electrons. The θ dependence of TMR exhibits the conventional spin-valve effect, i.e., the conductance is larger in the antiparallel configuration than that in the parallel configuration for larger η. A small η (for example $\eta < 0.7$) implies that $\Gamma_\uparrow < \Gamma_\downarrow$ (i.e. the tunneling probability of electrons from the spin up subband to spin up subband is less than that from down to down subbands), leading to an inverse TMR (i.e. the conductance in the antiparallel case is larger than that in the parallel case), as shown in Fig. 2(b). When η is around 0.65, the TMR is negligibly small and displays a nonmonotonic behavior, as shown in Fig. 2(c). It suggests that the coupling strength of the spin subbands leads to the nonmonotonic change of the TMR. When the polarization $P = 1$, i.e. if the leads are made of half-metals, the $TMR(\theta)$ will be always positive, and $TMR(\pi) = 1$, which recovers the perfect spin-valve effect. Here it should be pointed out that Bratkovsky[25] has considered a resonant tunnel diode (RTD) with electrons tunneling through a single-impurity level which is similar to the present structure, where, by invoking a different method, the θ- and bias-dependences of the conductance were obtained. However, the asymmetry of the tunneling rates $\Gamma_{\uparrow(\downarrow)}$ was not considered there while it is included in the present case, which gives rise to interesting behaviors, as manifested in Fig. 2.

The effect of the spin polarization P of the leads on the ETC as well as the $TMR(\theta)$ as a function of θ is presented in Figs. 3(a) and (b). It can be seen that the ETC and the $TMR(\theta)$ are affected considerably by P. At $\theta = \pi/2$, there is a crossing point on the curve of the ETC, showing that the ETC, thus the tunnel conductance, does not depend on the polarization when the magnetic moments of the leads are aligned perpendicular. As $\theta < \pi/2$, the ETC increases with increasing the polarization at a given θ; when $\theta > \pi/2$, the ETC decreases with increasing the polarization, as shown in Fig. 3(a). This is easy to understand, because $T_{eff}(\theta) \sim 1 + P^2 \cos\theta$. When $P = 1$ and $\theta = \pi$, the ETC is zero, showing again a spin-valve phenomenon. This is because in this situation the majority (spin-up) subband of the left lead is fully filled, while the minority (spin-down) subband is empty, if the spin-flip scattering is ignored in the tunneling process, the transport of the minority electrons in the left lead tunneling into the minority subband of the right lead is prohibited[34]. At a given θ, $TMR(\theta)$ increases with increasing the polarization P, as shown in Fig. 3(b). This behavior can be simply understood by the fact $TMR(\theta) \sim [2P^2/(1+P^2)] \sin^2\theta/2$.

To be consistent with the common definition of the TMR in literature, we define a quantity $TMR = 1 - C_{AP}/C_P$,

where C_{AP} is the tunnel conductance when the magnetizations of the ferromagnets are aligned antiparallel. In fact, such a definition is nothing but $TMR(\theta = \pi) = TMR$. In Fig. 4, we show the TMR as a function of the incident energy of electrons. It can be observed that the TMR reveals different behaviors for different η. First, for any η there is a peak at $E = \varepsilon_0$, and the curves have two crossing points at $E = E_1$ and E_2, suggesting that the TMR at $E = \varepsilon_0$, E_1 and E_2 is independent of η. This property may be caused by the resonant tunneling. Second, when $E < E_1$ and $E > E_2$, the TMR changes from negative to positive with increasing η, and larger η, larger the TMR; when $E_1 < E < E_2$ except $E = \varepsilon_0$, larger η, smaller the TMR. It is obvious that the TMR is symmetrical to the axis $E = \varepsilon_0$. This is a characteristic of the resonant tunneling structure.

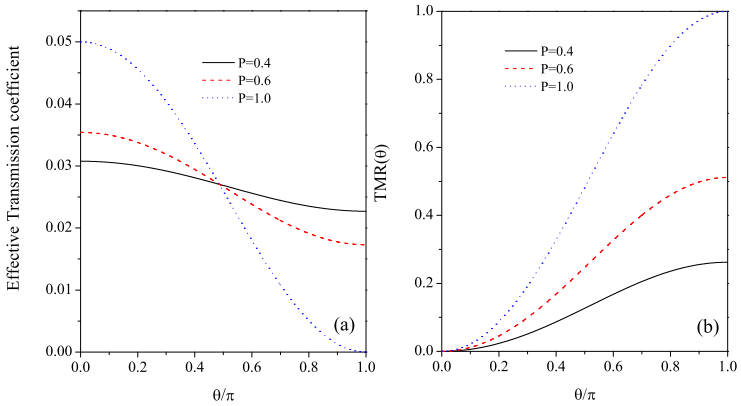


FIG. 3: (Color online) The ETC (a) and the $TMR(\theta)$ (b) as a function of θ for different polarization P. The parameters are taken as $\eta = 1.0$, $\varepsilon_0 = 5$, $E_f = 8$.

So far, we have discussed the spin-dependent transport of the structure at zero temperature. Let us now look at what happens at finite but low temperature. To proceed, we set $\mu_L - \mu_R = eV$ and $\mu_L = 0$. In the rest of this subsection, we follow the treatment of Rudziński and Barnaś[26], and consider the bias-dependent energy level of the central region as $\varepsilon_d = \varepsilon_0 - xeV$, where $x = d_L/(d_L + d_R)$, $0 < x < 1$, d_L and d_R are the thickness of the left and the right barrier. This treatment is corresponding to introduce a constant Hartree potential in the central scattering region as discussed in Ref.[35]. As the structure under consideration is symmetrical, we have $x = 1/2$ in the present case. The dc bias dependence of the current and the differential conductance is depicted in Figs. 5(a) and (b). (Note that throughout this paper any voltage is all scaled by Γ/e.) It can be observed that the current increases with increasing dc bias for different energy level of the central region. When $\varepsilon_0 = 0$, the current is a monotonic function of V; when ε_0 becomes larger, the curvature of the current alters with V, and the current rises dramatically at $V = \frac{2\varepsilon_0}{e}$ to saturation, as displayed in Fig. 5(a). As the energy of the central spacer is presumed to be positive, its role is like a barrier. Thus, one may see that with increasing ε_0 the current is remarkably suppressed. When the external dc bias lifts the Fermi level of the left lead to meet with the resonant energy level, the resonance may occur, which causes the current rapidly rising around the resonant position. This character can be clearly seen in Fig. 5(b), in which the differential conductance exhibits resonant peaks at $\varepsilon_0 = \frac{1}{2}eV$, i.e. $\varepsilon_d = 0$, a typical character of the resonant tunneling. At low bias, the differential conductance exhibits an ohmic behavior especially for large ε_0, i.e., is independent of the bias voltage; as V goes higher, the conductance deviates the ohmic behavior, which is more obvious when ε_0 is small. Since the appearance of the resonant tunneling, the overall behavior of the different conductance in this junction structure differs dramatically from the classical behavior, as manifested in Fig. 5(b). The TMR as a function of the dc bias voltage for different ε_0 is shown in Fig. 6. It is found that the TMR decreases with increasing dc bias at low bias but increases at high bias. This feature is consistent with the experimental observation[36] although the system investigated in the experiment is a single-barrier structure. One may note that for $\varepsilon_0 = 2$ or 5 the TMR first decreases to a minimum, then slowly rises with the dc bias. Before reaching the minimum, there is a "shoulder" structure for the TMR. This behavior is also noted by Wang et al.[35], in which they attribute it to the quantum resonance. In the present case we believe that it may be caused by the coupling between the central region and the leads. This coupling makes the sharp energy levels in the central region extended to those with a finite width, leading to that the electrons in the central region can relax to the leads. It may be the finite width of the energy levels in

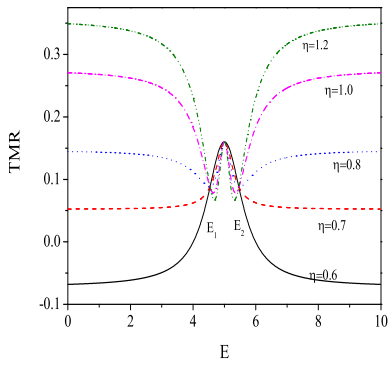


FIG. 4: (Color online) The TMR versus energy E for different η. The parameters are taken as $P = 0.4$, $\varepsilon_0 = 5$.

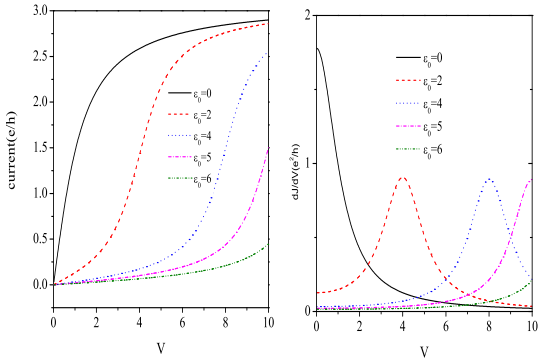


FIG. 5: (Color online) The external bias voltage dependence of the current (a) and the differential conductance (b), where $P = 0.4$, $\eta = 1.0$, $k_BT = 0.1\Gamma$, $\theta = \pi/3$.

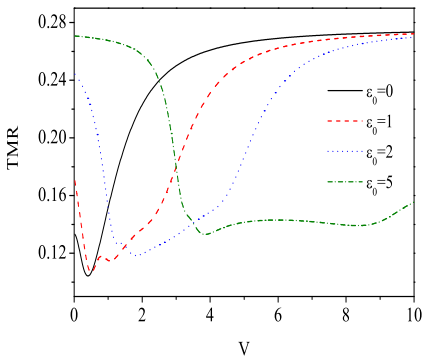


FIG. 6: (Color online) The TMR versus the dc bias voltage. The parameters are taken the same as in Fig. 5.

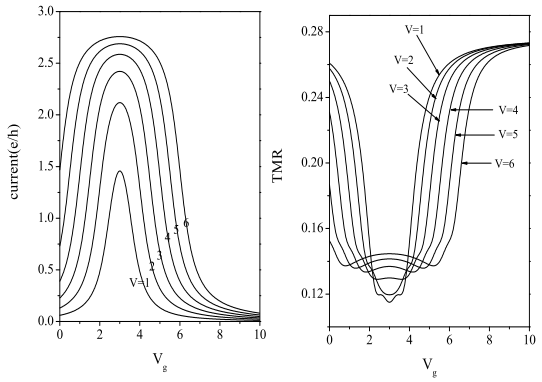


FIG. 7: The Current (a) and the TMR (b) versus gate voltage V_g for different external dc bias voltages, where $P = 0.4$, $\varepsilon_0 = 3$, $\eta = 1.0$, $k_BT = 0.1\Gamma$, and $\theta = \pi/3$ in (a).

the central region that results in the "shoulder" structure. In practice, the energy levels in the central region can be tuned by applying a gate voltage V_g. We may assume that the energy levels in the central region can be modulated in a form of $\varepsilon_d = \varepsilon_0 - xeV - V_g$. The dependence of the current and the TMR on the gate voltage V_g for different bias voltages is depicted in Fig. 7, where $\varepsilon_0 = 3$. It can be observed that with increasing gate voltage the current first rises rapidly, and goes to the maximum at $V_g = \varepsilon_0$, then decreases rapidly towards zero, as shown in Fig. 7(a). For a large V, the current shows a hump behavior. It can be understood as follows. When a dc bias V is applied to the leads, the Fermi energies of the left and the right leads are split by eV, i.e. $E_f^L - E_f^R = eV$. When the resonant energy level ε_d is in the region $E_f^R < \varepsilon_d < E_f^L$, the resonant energy level provides a tunneling channel and the resonance occurs, leading to that the current increases rapidly; when $\varepsilon_d > E_f^L$, the energy level in the central spacer serves as a barrier and the current decreases with increasing V_g. When the dc bias becomes larger, the width of the resonant peaks become wider, giving rise to a hump behavior. The gate voltage dependence of the TMR is shown in Fig. 7(b). When the gate voltage is small, for instance $V = 1$, the TMR goes to the minimum at $V_g = \varepsilon_0$ where the resonant peaks of the current just appear. Around the minimum of the TMR, there appear two "shoulders" on both sides of $V_g = \varepsilon_0$ for different V. When V becomes larger, the "shoulder" becomes flatter. With increasing the external dc bias voltage, the minimum of the TMR becomes a round peak while the "shoulders" become two minima. The origin

of the shoulder behavior is the same as that explained above.

B. Three-Terminal Device Under a dc Bias

Now we turn to discuss a three-terminal device under a dc bias. The multi-terminal device has been extensively investigated within a framework of the mesoscopic device. For instance, a three-terminal device was discussed in terms of the Landauer-Büttiker scattering matrix theory (SMT)[18], where a third terminal is introduced to measure the chemical potential μ_3 and the current flowing out of it is set to zero, say, $j_3 = 0$. In this way, the chemical potential of the third terminal can be expressed in terms of the chemical potentials of the first and the second terminals. When electrons enter into the third terminal and then flow out of it into the scattering region, their phases are randomized. For a spin-dependent three-terminal device, Johnson[15] observed the spin bottleneck effect in a spin transistor. In a structure such as a FM/NM/FM multilayer, the polarized current is injected from one of the FM layers into the NM layer and flows out of it; the other FM layer and the NM layer serve as a voltmeter to give a voltage output which depends on the magnetization configurations of the two ferromagnets. Johnson and Silsbee[37] proposed the nonequilibrium thermodynamic theory to investigate the charge transport and the nonequilibrium magnetization. Fert and Lee[16] investigated Johnson's spin transistor device and discussed the effect of junction resistance on the spin accumulation based on the Boltzmann equation. Brataas et al.[19, 20] extended the SMT to a ferromagnetic three-terminal system FM/NM/FM, where the current flows from the first FM terminal into the NM spacer region, then into a second FM terminal, but the net current flowing out of the third FM terminal is set to zero. When the magnetizations in the first and the second FM terminals are antiparallel, the current flowing through the first and second terminals can be varied with the magnetization direction of the third FM terminal through which there is no net current flowing, though. When the magnetization in the third terminal $\mathbf{M}_3$ deviates by $\pi/2$ to the first one $\mathbf{M}_1$, the current goes to its maximum. Here we propose a three-terminal spintronic device which is somewhat different

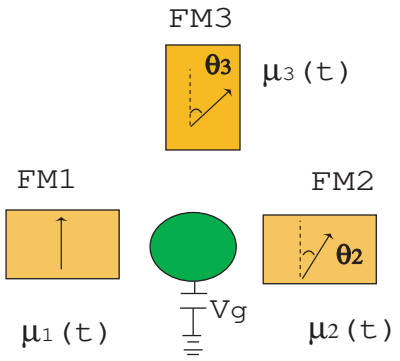


FIG. 8: (Color online) The schematic layout of the resonant tunneling structure with three ferromagnetic terminals.

from the one discussed in Refs.[19, 20]. We suppose that the third FM terminal is applied by an external dc bias too, enabling the net current to flow through it, just like a usual semiconductor transistor. We call it a spin transistor with source, whose schematic layout is shown in Fig. 8. In the following, we shall investigate the spin-dependent electrical transport in such a STS.

From Eq.(25), the current of the αth lead is

$$J_\alpha^c = \frac{e}{\hbar}\sum_{\beta\neq\alpha}\int\frac{d\omega}{2\pi}[f_\alpha(\omega) - f_\beta(\omega)]Tr_\sigma[\mathbf{\Gamma}_\alpha\mathbf{G}_d^r(\omega)\mathbf{\Gamma}_\beta\mathbf{G}_d^a(\omega)], \tag{34}$$

where β runs over the other leads besides α. We re-arrange the current flowing in the leads as a vector form:

$$\overrightarrow{J} = \mathbf{D}\overrightarrow{u}, \tag{35}$$

$$\overrightarrow{J} = \begin{pmatrix} J_1 \\ J_2 \\ J_3 \end{pmatrix},$$

with

$$\overrightarrow{u} = \begin{pmatrix} 1 \\ 1 \\ 1 \end{pmatrix}$$

a constant vector, and

$$\mathbf{D} = \mathbf{fC} - \mathbf{Cf} = \frac{e}{\hbar}\int \frac{d\omega}{2\pi} \begin{pmatrix} 0 & (f_1 - f_2)C_{12} & (f_1 - f_3)C_{13} \\ (f_2 - f_1)C_{21} & 0 & (f_2 - f_3)C_{23} \\ (f_3 - f_1)C_{31} & (f_3 - f_2)C_{32} & 0 \end{pmatrix},$$

where

$$\mathbf{f} = \begin{pmatrix} f_1 & 0 & 0 \\ 0 & f_2 & 0 \\ 0 & 0 & f_3 \end{pmatrix}$$

with $f_{1(2,3)} = f_{1(2,3)}(\omega)$, and

$$\mathbf{C} = \begin{pmatrix} 0 & C_{12} & C_{13} \\ C_{21} & 0 & C_{23} \\ C_{31} & C_{32} & 0 \end{pmatrix},$$

where the matrix elements are given by $C_{\alpha\beta} = Tr_\sigma[\mathbf{\Gamma}_\alpha \mathbf{G}_d^r(\omega)\mathbf{\Gamma}_\beta \mathbf{G}_d^a(\omega)]$ with α, β the indices of the leads. In general, the formulas can be extended to the system with N terminals, and the current will be a vector with N dimensions where $\mathbf{C}$ is a $N \times N$ matrix. When one or some of the N terminals are made of NM, then $P = 0$ and the tunneling matrix reduces to a number. In the present assumption, $\mathbf{C}$ is a symmetrical matrix, i.e. $C_{12} = C_{21}$, $C_{13} = C_{31}$, and $C_{23} = C_{32}$.

In the subsequent discussion, we call the parallel (antiparallel) configuration when the magnetizations of the first and second terminals are parallel (antiparallel). We set the angle between the magnetizations of the third terminal and the first one is θ, as indicated in Fig. 8. Then, the current flowing through the second terminal is

$$\begin{aligned} J_2^{c,P} &= \frac{e}{\hbar}\int \frac{d\omega}{2\pi}\{[f_2(\omega) - f_1(\omega)]Tr_\sigma[\mathbf{\Gamma}_2^P \mathbf{G}_d^{r,P}(\omega)\mathbf{\Gamma}_1 \mathbf{G}_d^{a,P}(\omega)] \\ &\quad + [f_2(\omega) - f_3(\omega)]Tr_\sigma[\mathbf{\Gamma}_2^P \mathbf{G}_d^{r,P}(\omega)\mathbf{\Gamma}_3 \mathbf{G}_d^{a,P}(\omega)]\}, \end{aligned} \tag{36}$$

where the superscript P means the parallel configuration. In the antiparallel configuration, the current flowing through the second terminal is

$$\begin{aligned} J_2^{c,AP} &= \frac{e}{\hbar}\int \frac{d\omega}{2\pi}\{[f_2(\omega) - f_1(\omega)]Tr_\sigma[\mathbf{\Gamma}_2^{AP} \mathbf{G}_d^{r,AP}(\omega)\mathbf{\Gamma}_1 \mathbf{G}_d^{a,AP}(\omega)] \\ &\quad + [f_2(\omega) - f_3(\omega)]Tr_\sigma[\mathbf{\Gamma}_2^{AP} \mathbf{G}_d^{r,AP}(\omega)\mathbf{\Gamma}_3 \mathbf{G}_d^{a,AP}(\omega)]\}, \end{aligned} \tag{37}$$

where the superscript AP means the antiparallel configuration. At low temperature and small bias voltage, the difference of the conductance in these two configurations can be obtained by

$$\begin{aligned} \triangle C &= C_2^P(\theta_3 = \theta) - C_2^{AP}(\theta_3 = \theta) \\ &= \frac{e^2}{\hbar} Tr_\sigma[(G^{a,P}\mathbf{\Gamma}_2^P \mathbf{G}_d^{r,P}(\omega) - \mathbf{G}_d^{a,AP}(\omega)\mathbf{\Gamma}_2^{AP}\mathbf{G}_d^{r,AP}(\omega))(\mathbf{\Gamma}_1 + \mathbf{\Gamma}_3)], \end{aligned} \tag{38}$$

Define the $TMR(\theta_3)$ as usual

$$\begin{aligned} TMR(\theta_3) &= \frac{\triangle C}{C_2^P(\theta_3 = 0)} \\ &= \frac{Tr_\sigma[(\mathbf{G}^{a,P}(E_f)\mathbf{\Gamma}_2^P \mathbf{G}_d^{r,P}(E_f) - \mathbf{G}_d^{a,AP}(E_f)\mathbf{\Gamma}_2^{AP}\mathbf{G}_d^{r,AP}(E_f))(\mathbf{\Gamma}_1 + \mathbf{\Gamma}_3)]}{Tr_\sigma[\mathbf{\Gamma}_2^P \mathbf{G}_d^{r,P}(E_f, \theta_3 = 0)\mathbf{\Gamma}_1 \mathbf{G}^{a,P}(E_f, \theta_3 = 0)]}. \end{aligned} \tag{39}$$

We shall consider the STS device at finite temperature. The terminal current is determined by $J_\alpha = -e\left\langle \dot{N}_\alpha \right\rangle$. Negative J_α indicates that the positive charges tunnel through the barrier and enter into the central region (i.e. the electrons tunnel through the barrier from the central region to the leads), and the minus means the reduction of the positive charges (i.e. the increase of the negative charges) in the αth terminal. When J_α is positive, the things become opposite. For simplicity, we set $\mu_1 = \mu_3$ and $\mu_1 - \mu_2 = eV$, while choose $\mu_2 = 0$. In this case, the electrons flow from the first and third terminals to the second terminal, suggesting that the positive charges tunnel through the barrier into the central region, and J_2^c is negative. As the flowing direction of the positive charges is the current direction, and noting $J_1^c + J_2^c + J_3^c = 0$, i.e. $J_1^c + J_3^c = -J_2^c$, we define the current flowing from the first and third terminal into the second terminal as

$$\begin{aligned} J_2(\theta_3 &= \theta) = \frac{1}{2}(J_1^c + J_3^c - J_2^c) \\ &= \frac{e}{2\hbar}\int \frac{d\omega}{2\pi}[f_1(\omega) - f_2(\omega)]\{Tr_\sigma[(\mathbf{\Gamma}_1 + \mathbf{\Gamma}_3)\mathbf{G}_d^r(\omega)\mathbf{\Gamma}_2\mathbf{G}_d^a(\omega)] \\ &\quad + Tr_\sigma[\mathbf{\Gamma}_2\mathbf{G}_d^r(\omega)(\mathbf{\Gamma}_1 + \mathbf{\Gamma}_3)\mathbf{G}_d^a(\omega)]\}. \end{aligned} \tag{40}$$

Based on this equation, we could obtain the current $J_{2,P(AP)}(\theta_3 = \theta)$ at the parallel (antiparallel) configuration numerically.

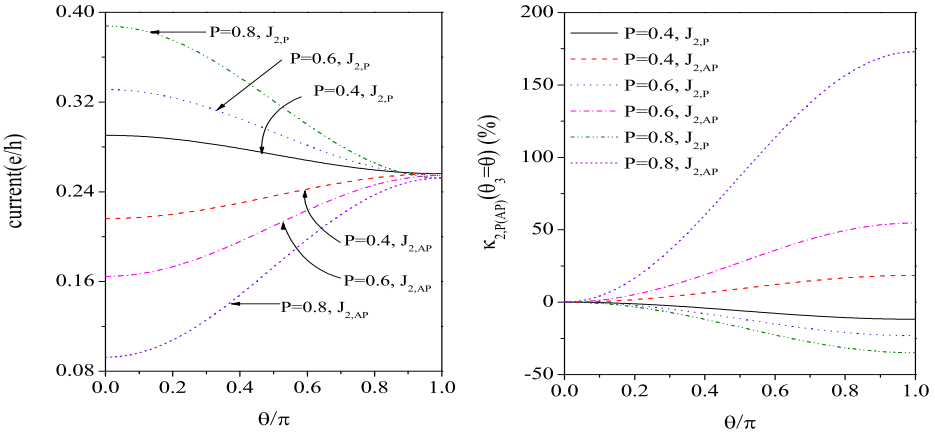


FIG. 9: (Color online) The θ dependence of the current (a) and the current ratio $\kappa_{2,P(AP)}$ (b) for different polarizations and magnetization configurations (parallel and antiparallel). The parameters are taken as $V = 5$, $\varepsilon_0 = 8$, $k_BT = 0.1\Gamma$, $\eta = 1.0$.

The θ dependence of $J_{2,P(AP)}(\theta_3 = \theta)$ under different polarizations is shown in Fig. 9(a), where the parameters are assumed the same as those in the proceding subsection, the temperature is taken as $k_BT = 0.1\Gamma$, and the three terminals are supposed to be made of the same ferromagnets. In the parallel configuration, the current $J_{2,P}(\theta_3 = \theta)$ decreases with increasing θ. This is because of the spin-valve effect, the current flowing from the third terminal into the second terminal decreases with increasing θ, leading to the total current into the second terminal decreases with increasing θ. While in the antiparallel case, the current flowing from the third terminal into the second terminal increases with increasing θ because $\mathbf{M}_3$ rotates from the antiparallel to parallel configuration with respect to $\mathbf{M}_2$, resulting in that the total current of the second terminal increases with θ. We note that the current in the antiparallel configuration is equal to that in the parallel configuration when $\theta = \pi$. Because in this case, i.e. the magnetizations of the first and third terminals are antiparallel, the state of $\mathbf{M}_2 \parallel \mathbf{M}_1$ but $\mathbf{M}_3$ antiparallel to $\mathbf{M}_2$ is symmetrical to the state of $\mathbf{M}_2 \parallel \mathbf{M}_3$ but $\mathbf{M}_2$ antiparallel to $\mathbf{M}_1$, the current in the two states are equal, and the TMR would be zero. Besides, we find that regardless of the magnetization configuration, the polarization makes the absolute value of the current increases except $\theta = \pi$.

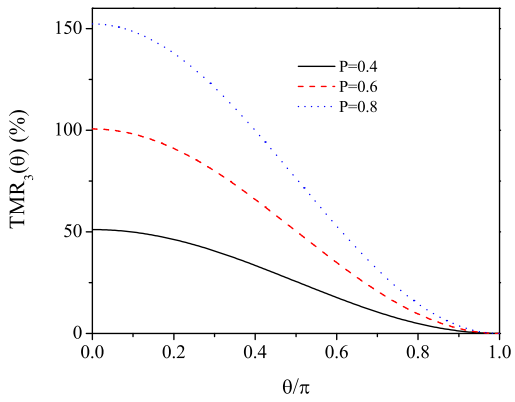


FIG. 10: (Color online) The θ dependence of the $TMR_3(\theta)$ of the three-terminal device for different polarizations. The parameters are the same as those in Fig. 9.

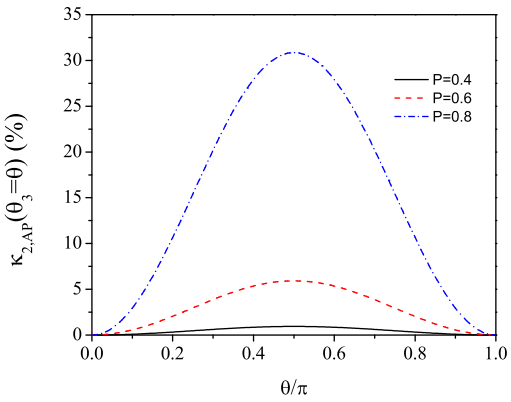


FIG. 11: (Color online) The current ratio versus θ for the antiparallel configuration at different polarizations. The parameters are taken as $V = 5$, $\varepsilon_0 = 8$, $k_BT = 0.1\Gamma$, $\eta = 1.0$.

To illustrate the effect of the tunnel magnetoresistance, for this three-terminal device we define the current ratio as

$$\kappa_{2,P(AP)}(\theta_3 = \theta) = \frac{J_{2,P(AP)}(\theta_3 = \theta) - J_{2,P(AP)}(\theta_3 = 0)}{J_{2,P(AP)}(\theta_3 = 0)}. \tag{41}$$

This quantity reflects the relative change of the tunnel current with respect to the change of the magnetization configuration, whose role is similar to the TMR. The angle dependence of the current ratio $\kappa_{2,P(AP)}(\theta)$ for the second terminal is shown in Fig. 9(b). It can be noted that $\kappa_{2,P}(\theta)$ is negative for the parallel configuration and the absolute value of $\kappa_{2,P}(\theta)$ increases with increasing θ. For the antiparallel configuration, $\kappa_{2,AP}(\theta)$ is positive and increases with increasing θ. $\kappa_{2,AP}(\pi)$ is larger than the absolute value of $\kappa_{2,P}(\pi)$. This difference becomes larger for a larger polarization. For example, $P = 0.8$, $\kappa_{2,AP}(\pi) \approx 173\%$, $\kappa_{2,P}(\pi) \approx -35\%$. It suggests that the change of the current for the antiparallel configuration is larger than for the parallel configuration. So, the current flowing out of the second terminal can be enlarged or reduced by changing the relative orientation of the magnetic moments of the third terminal. The so-obtaind current amplification effect is considerably large for a larger polarization at the antiparallel configuration. For example, $P = 0.6$, the change of the current ratio can be as high as 55%. Such a current amplification effect is quite different from that in a usual semiconductor transistor. The present results show that in a STS, by merely changing the magnetization direction of the third terminal the current flowing through the first and second terminals can be amplified or reduced. Besides, we can define another current ratio, $TMR_3(\theta)$, for the STS to investigate the change of the current flowing out of the second terminal when the magnetization configuration varies from parallel to antiparallel:

$$TMR_3(\theta) = \frac{J_{2,P}(\theta) - J_{2,AP}(\theta)}{J_{2,P}(0)}. \tag{42}$$

The θ dependence of the $TMR_3(\theta)$ for different polarizations is shown in Fig. 10. One may see that the TMR decreases with increasing θ. As mentioned above, the states of the parallel and antiparallel configuration are symmetrical at $\theta = \pi$, leading to the currents equal, and then giving rise to the $TMR_3(\pi)$ zero. When the polarization is larger, the TMR becomes larger.

Here we would like to point out that the present three-terminal device is different from that discussed by Brataas et al.[19, 20]. In their device, the third terminal is introduced as an inelastic scattering resource, and there is no net current flowing through this terminal. In the present STS device, there is net current flowing through the third terminal, and the chemical potential of the third terminal is not changed (i.e. its chemical potential cannot be expressed in terms of that of the first and second terminals). Owing to the spin-dependent scatterings, we have found that the current flowing out of the second terminal can be enlarged by changing θ when the magnetization

configuration of the first and second terminals is antiparallel. The enlargement is more remarkable with increasing polarization. This three-terminal device is similar to the usual semiconductor transistor. In the latter case, the current flowing out of the collector is enlarged by varying the voltage bias between the emitter and the base, while in the present case the enlargement of the current can be realized by changing the direction of the magnetization of the third terminal. This is of course of the quantum-mechanical origin. Another difference between our device and that of Brataas et al. is that the current can be modified in a STS by changing θ at the parallel configuration, but it cannot be tuned in the case of Refs.[19, 20].

However, the result presented in Refs.[19, 20] can be recovered from our analysis. Suppose that there is no net current flowing through the third terminal in the STS, like the treatment of Büttiker. This implies that the chemical potential of the third terminal μ_3 can be determined by the chemical potentials of the other two terminals. As a result, we get

$$J_2(\theta_3=\theta)=\frac{e}{2\hbar}\int\frac{d\omega}{2\pi}[f_1(\omega)-f_2(\omega)]\frac{C_{12}(C_{13}+C_{23})+C_{13}C_{23}}{C_{13}+C_{23}}. \tag{43}$$

In addition, it is assumed that $-V/2$ is applied to the first terminal and $V/2$ to the second terminal. The current ratio $\kappa_{2,P(AP)}(\theta)$ can be obtained in terms of Eq. (43), and the result is shown in Fig. 11. One may find that our result is fairly consistent with that shown in Refs.[19, 20], although quite different methods are used.

IV. TWO-TERMINAL DEVICE UNDER AN AC BIAS

A. General Formulation

Let us turn to investigate the spin-dependent transport in the magnetic tunnel junction with two terminals under an ac bias, where the noncollinear configuration of magnetizations of the FM leads is presumed. Under an ac bias, the total current of each terminal is a sum of the "terminal current" and the "displacement current" with the ac bias determined by Eqs.(15) and (16). The total current is

$$J=\frac{1}{2}(J_L-J_R)=\frac{1}{2}[(J_L^c-J_R^c)+(J_L^d-J_R^d)]. \tag{44}$$

Again, we need to calculate the function $\mathbf{A}_\alpha(\omega,t)$. From Eq.(23), we have

$$\begin{aligned}\mathbf{A}_\alpha(\omega,t) &= \int_{-\infty}^{t}dt'\int\frac{d\omega''}{2\pi}e^{i(\omega-\omega'')(t-t')}e^{i\int_{t'}^{t}dt''[V_\alpha\cos(\omega_\alpha t'')-V_0\cos(\omega_0 t'')]}\mathbf{G}_d^r(\omega'')\\ &= i\sum_{mnm'n'}J_\alpha\binom{mn}{m'n'}\int\frac{d\omega''}{2\pi}\frac{\mathbf{G}_d^r(\omega'')e^{-i[(m-n)\omega_\alpha+(m'-n')\omega_0]t}}{\omega-\omega''+m\omega_\alpha-n'\omega_0+i0^+},\end{aligned} \tag{45}$$

with $J_\alpha\binom{mn}{m'n'}=J_m(\frac{V_\alpha}{\omega_\alpha})J_n(\frac{V_\alpha}{\omega_\alpha})J_{m'}(\frac{V_0}{\omega_0})J_{n'}(\frac{V_0}{\omega_0})$, where use has been made of $e^{ix\sin\zeta}=\sum_{m=-\infty}^{\infty}J_m(x)e^{im\zeta}$ with $J_m(x)$ is the m-th order Bessel function. In the same way, we can get

$$\begin{aligned}\mathbf{A}_\alpha(\omega,t)\mathbf{\Gamma}_\alpha\mathbf{A}_\alpha^\dagger(\omega,t) &= \sum_{mnm'n'}J_\alpha\binom{mn}{m'n'}\int\frac{d\omega'}{2\pi}\frac{d\omega''}{2\pi}\mathbf{G}_d^r(\omega'')\mathbf{\Gamma}_\alpha\mathbf{G}_d^a(\omega')\cdot\\ &\quad\frac{e^{-i[(m-n)\omega_\alpha+(m'-n')\omega_0]t}}{(\omega-\omega''+m\omega_\alpha-n'\omega_0+i0^+)(\omega-\omega'+n\omega_\alpha-m'\omega_0-i0^+)}.\end{aligned} \tag{46}$$

The time-average of a time-dependent physical quantity $F(t)$ is defined by

$$\langle F(t)\rangle=\lim_{T\to\infty}\frac{1}{T}\int_{-T/2}^{T/2}F(t)dt. \tag{47}$$

The time-averaged displacement current can be in principle obtained by means of Eqs.(28) and (46). Although the integral on time can be nonzero only when the term in the square bracket of the exponent in Eq.(46) is zero, to get

the displacement current a differential of Eq.(46) with respect to t should be made, leading to that the time-averaged displacement current is zero. This is also mentioned in Ref.[31]. If $F(t)$ is a periodic function of time, its integral over time should be finite. When T tends to infinity, the time-averaged $F(t)$ will be zero. When $(n'-m')\omega_0=(m-n)\omega_\alpha$ holds, the first term of the time-averaged αth terminal current in Eq.(25) is

$$\langle J_\alpha^c(t)\rangle^{(1)}=\frac{e}{\hbar}\Re e\sum_{mnm'n'}J_\alpha(^{mn}_{m'n'})\int\frac{d\omega'}{2\pi}\frac{d\omega''}{2\pi}\frac{2f_\alpha(\omega)Tr_\sigma[\mathbf{\Gamma}_\alpha\mathbf{G}_d^r(\omega'')]}{(\omega''-\omega-m\omega_\alpha+n'\omega_0-i0^+)}, \tag{48}$$

and the second term is

$$\begin{aligned}\langle J_\alpha^c(t)\rangle^{(2)} &= \frac{2e}{\hbar}\Re e\sum_{mnm'n'\beta}J_\alpha(^{mn}_{m'n'})\int\frac{d\omega}{2\pi}\frac{d\omega'}{2\pi}\frac{d\omega''}{2\pi}f_\beta(\omega) \\ &\cdot\frac{Tr_\sigma[\mathbf{\Gamma}_\alpha\mathbf{G}_d^r(\omega'')\mathbf{\Gamma}_\beta\mathbf{G}_d^a(\omega')]}{(\omega''-\omega-m\omega_\alpha+n'\omega_0-i0^+)(\omega-\omega'+n\omega_\alpha-m'\omega_0-i0^+)}.\end{aligned} \tag{49}$$

The time-averaged terminal current is zero for other cases. To get $\langle J_\alpha^c(t)\rangle^{(1)}$, we shall perform the integral over ω'' first. By noting that the pole of $\mathbf{G}_d^r(\omega'')$ is on the lower-half plane, while the pole of the kernel function is on the upper-half plane $\omega''=\omega+m\omega_\alpha-n'\omega_0+i0^+$, we may perform a contour integral along the upper-half plane, and get

$$\langle J_\alpha^c(t)\rangle^{(1)}=-\frac{2e}{\hbar}\Im m\sum_{mnm'n'}J_\alpha(^{mn}_{m'n'})\int\frac{d\omega'}{2\pi}f_\alpha(\omega)Tr_\sigma[\mathbf{\Gamma}_\alpha\mathbf{G}_d^r(\omega,\varepsilon_0^\alpha(m,n'))], \tag{50}$$

where $\mathbf{G}_d^r(\omega,\varepsilon_0^\alpha(m,n'))=[\omega-\varepsilon_0^\alpha(m,n')+\frac{i}{2}\mathbf{\Gamma}]^{-1}$, and $\varepsilon_0^\alpha(m,n')=\varepsilon_0-m\omega_\alpha+n'\omega_0$. To evaluate $\langle J_\alpha^c(t)\rangle^{(2)}$, one should first perform the integral over ω'', then make a contour integral on the lower-half plane, and get

$$\begin{aligned}\langle J_\alpha^c(t)\rangle^{(2)} &= -\frac{e}{\hbar}\Re e\sum_{mnm'n'\beta}J_\alpha(^{mn}_{m'n'})\int\frac{d\omega}{2\pi}f_\beta(\omega)Tr_\sigma\{\mathbf{\Gamma}_\alpha\mathbf{G}_d^r(\omega,\varepsilon_0^\beta(m,n')) \\ &\cdot\mathbf{\Gamma}_\beta\mathbf{G}_d^a(\omega,\varepsilon_0^\beta(n,m'))\},\end{aligned} \tag{51}$$

where $\mathbf{G}_d^a(\omega,\varepsilon_0^\beta(n,m'))=[\omega-\varepsilon_0^\beta(n,m')-\frac{i}{2}\mathbf{\Gamma}]^{-1}$. As $(n'-m')\omega_0=(m-n)\omega_\alpha$, leading to $\varepsilon_0^\beta(m,n')=\varepsilon_0^\beta(n,m')$, we write $\varepsilon_0^\beta(m,n')$ as ε_0^β. After some algebra, the time-averaged current of the αth terminal can be obtained

$$\begin{aligned}\langle J_\alpha^c(t)\rangle &= \frac{e}{\hbar}\sum_{mnm'n'}\int\frac{d\omega}{2\pi}Tr_\sigma\{[J_\alpha(^{mn}_{m'n'})f_\alpha(\omega)\mathbf{\Gamma}_\alpha\mathbf{G}_d^r(\omega,\varepsilon_0^\alpha)\mathbf{\Gamma}\mathbf{G}_d^a(\omega,\varepsilon_0^\alpha)] \\ &-[\sum_\beta J_\beta(^{mn}_{m'n'})f_\beta(\omega)\mathbf{\Gamma}_\alpha\mathbf{G}_d^r(\omega,\varepsilon_0^\beta)\mathbf{\Gamma}_\beta\mathbf{G}_d^a(\omega,\varepsilon_0^\beta)]\},\end{aligned} \tag{52}$$

For the time-averaged displacement current is zero, by noting $\langle J\rangle=\frac{1}{2}(\langle J_L^c(t)\rangle-\langle J_R^c(t)\rangle)$, one may obtain

$$\begin{aligned}\langle J_\alpha^c(t)\rangle &= \frac{e}{2\hbar}\sum_{mnm'n'}\int\frac{d\omega}{2\pi}\{J_L(^{mn}_{m'n'})f_L(\omega)(Tr_\sigma[\mathbf{\Gamma}_L\mathbf{G}_d^r(\omega,\varepsilon_0^L)\mathbf{\Gamma}_R\mathbf{G}_d^a(\omega,\varepsilon_0^L)] \\ &+Tr_\sigma[\mathbf{\Gamma}_R\mathbf{G}_d^r(\omega,\varepsilon_0^L)\mathbf{\Gamma}_L\mathbf{G}_d^a(\omega,\varepsilon_0^L)]) \\ &-J_R(^{mn}_{m'n'})f_R(\omega)(Tr_\sigma[\mathbf{\Gamma}_R\mathbf{G}_d^r(\omega,\varepsilon_0^R)\mathbf{\Gamma}_L\mathbf{G}_d^a(\omega,\varepsilon_0^R)] \\ &+Tr_\sigma[\mathbf{\Gamma}_L\mathbf{G}_d^r(\omega,\varepsilon_0^R)\mathbf{\Gamma}_R\mathbf{G}_d^a(\omega,\varepsilon_0^R)])\}.\end{aligned}$$

Define $\mathbf{M}=\mathbf{\Gamma}_L\mathbf{G}_d^r\mathbf{\Gamma}_R\mathbf{G}_d^a$, then $\mathbf{M}^T=(\mathbf{G}_d^a)^T(\mathbf{\Gamma}_R)^T(\mathbf{G}_d^r)^T(\mathbf{\Gamma}_L)^T$. Because $\mathbf{\Gamma}_L$, $\mathbf{\Gamma}_R$, $\mathbf{G}_d^r$ and $\mathbf{G}_d^a$ are all symmetrical matrices, we find $\mathbf{M}^T=\mathbf{G}_d^a\mathbf{\Gamma}_R\mathbf{G}_d^r\mathbf{\Gamma}_L$. With this observation, we get

$$\begin{aligned}\langle J\rangle &= \frac{e}{\hbar}\sum_{mnm'n'}\int\frac{d\omega}{2\pi}\{J_L(^{mn}_{m'n'})f_L(\omega)Tr_\sigma[\mathbf{\Gamma}_L\mathbf{G}_d^r(\omega,\varepsilon_0^L)\mathbf{\Gamma}_R\mathbf{G}_d^a(\omega,\varepsilon_0^L)] \\ &-J_R(^{mn}_{m'n'})f_R(\omega)Tr_\sigma[\mathbf{\Gamma}_R\mathbf{G}_d^r(\omega,\varepsilon_0^R)\mathbf{\Gamma}_L\mathbf{G}_d^a(\omega,\varepsilon_0^R)]\}.\end{aligned} \tag{53}$$

This is the time-averaged current of the system with two FM terminals whose magnetizations are arranged in a noncollinear configuration under an ac bias, which can be used to study the spin-dependent transport of the spin-polarized electrons in the presence of an ac field.

B. Photon-Assisted Spin-Dependent Resonant Tunneling

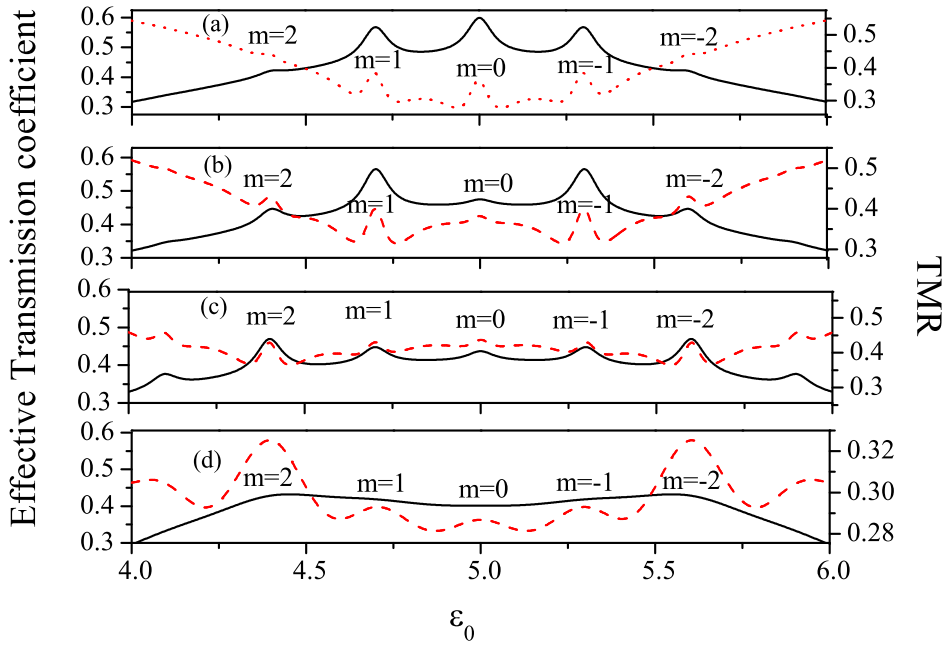


FIG. 12: (Color online) The ETC (solid lines) and TMR (dash lines) vary with the energy of the central spacer. Where $\alpha = V_0/\omega_0$, $\omega_0 = 0.3$, $P = 0.6$ and $E_f = 5$. (a) $\alpha = 1.4$ and $\eta = 10$; (b) $\alpha = 2$ and $\eta = 10$; (c) $\alpha = 3$ and $\eta = 10$; (d) $\alpha = 3$ and $\eta = 1$. The ETCs are calculated at $\theta = \pi/3$.

In this subsection, we shall consider a particular situation in which only a dc bias is applied between the two terminals while an ac bias voltage is applied to the central spacer region such as $\Delta_d(t) = V_0\cos(\omega_0 t)$. In this case, $J_L(^{mn}_{m'n'}) = J^2_{m'}(\frac{V_0}{\omega_0}) = J_R(^{mn}_{m'n'})$, $m' = n'$ and $\varepsilon_0^L = \varepsilon_0^R = \varepsilon_0 + m\omega_0 = \varepsilon_0'$. The time-averaged current becomes

$$\langle J\rangle = \frac{e}{\hbar}\sum_m \int \frac{d\omega}{2\pi} J_m^2(\frac{V_0}{\omega_0})[f_L(\omega) - f_R(\omega)]Tr_\sigma[\mathbf{\Gamma}_L\mathbf{G}_d^r(\omega,\varepsilon_0')\mathbf{\Gamma}_R\mathbf{G}_d^a(\omega,\varepsilon_0')], \tag{54}$$

where $J_m(\frac{V_0}{\omega_0})$ is the m-th order Bessel function. The effective transmission coefficient is given by $T_{eff} = \frac{1}{2}\sum_m J_m^2(\frac{V_0}{\omega_0})Tr_\sigma[\mathbf{\Gamma}_L\mathbf{G}_d^r(\omega,\varepsilon_0')\mathbf{\Gamma}_R\mathbf{G}_d^a(\omega,\varepsilon_0')]$. At low temperature and under a small dc bias, the integral can be performed by noting $\lim_{T\to 0, V_{dc}\to 0}(f_L(\omega) - f_R(\omega))/eV_{dc} = \delta(\omega - E_f)$. As a result, we can get the tunnel conductance $G = \frac{2e^2}{h}T_{eff}(E_f)$ as well as the $TMR = (G_P - G_{AP})/G_P$.

Based on these equations, the numerical calculation can be carried out. The parameters are taken as those in Sec. IIIA. The ETC and the TMR as a function of ε_0 is shown in Figs. 12(a)-(d). It is seen that the ETC and the TMR exhibit resonant peaks at certain values of ε_0, and the curves are symmetric to the axis $\varepsilon_0 = E_f$. These resonant peaks occur at the positions of the photonic sidebands characterized by $m = 0, \pm 1, \pm 2, ...$ which correspond to the shifts of the energy levels caused by the ac field in the central spacer. We have found that the resonant peaks of the ETC become sharper and higher as the orientations of the magnetizations of the left and the right ferromagnetic leads vary from antiparallel to parallel. With increasing θ, the amplitudes of the resonant peaks are noticed to become small. In addition, we have observed that the resonant magnitude of the ETC is sensitive to the ratio of the strength and the frequency of the ac field, say, $\alpha = V_0/\omega_0$, which appears as an argument of the Bessel function. With increasing α, the main resonant peak of the ETC at $\varepsilon_0 = E_f$ is suppressed, while more resonant peaks with large $|m|$ appear, as manifested in Figs. 12(a), (b) and (d). The resonant peaks of the TMR does not almost change with α. The ε_0

dependence of the ETC and the TMR for different η is presented in Figs. 12(c) and (d). One may observe that a small η suppresses the resonant peaks while broadens the peaks of the ETC and the TMR. With increasing η, the resonant peaks become more and obvious. In accordance with the definition, a larger η means that it is more difficult for the electrons with spin down to tunnel through the barrier and then into the leads, while it is easy for the electrons with spin up. So, the resonant peaks of the ETC become even sharper at smaller η in the antiparallel configuration, while the resonant peaks of the TMR become more obvious. One may note that there are several other peaks of the TMR besides the main resonance and the photonic sidebands as shown in Fig. 12(c), which are not caused by the additional resonant energy levels of the central region, but by the asymmetric factor of η on the spin-dependent transmission.

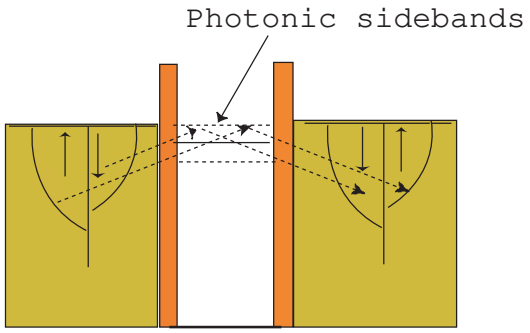


FIG. 13: (Color online) The schematic illustration of the photon-assisted tunneling. A very small dc bias is applied to the leads and an ac field is applied to the central spacer. The quantum well states in the central spacer will be modulated by the ac field. The dashed lines indicate the photonic sidebands besides the main resonance which is indicated by the solid line. In this illustration, only is the antiparallel configuration of the magnetizations of the left and the right ferromagnetic leads shown.

The tunneling process assisted by photons is schematically illustrated in Fig. 13. It can be seen that the photonic sidebands provide new channels for the electrons in the left ferromagnet to tunnel through the central spacer and into the right ferromagnet. Without the spin-flip scattering, the electrons with spin up (down) in the left will be accepted by the spin-up (-down) subband in the right. Because of the splitting of the energy bands of electrons with different spins, the spin-valve effect will appear. As ε_0 increases, the photonic sidebands with negative m, the main resonant energy level and the photonic sidebands with positive m pass through the Fermi level of the leads one by one. It is these additional channels from the photonic sidebands to make the ETC and the TMR be resonant.

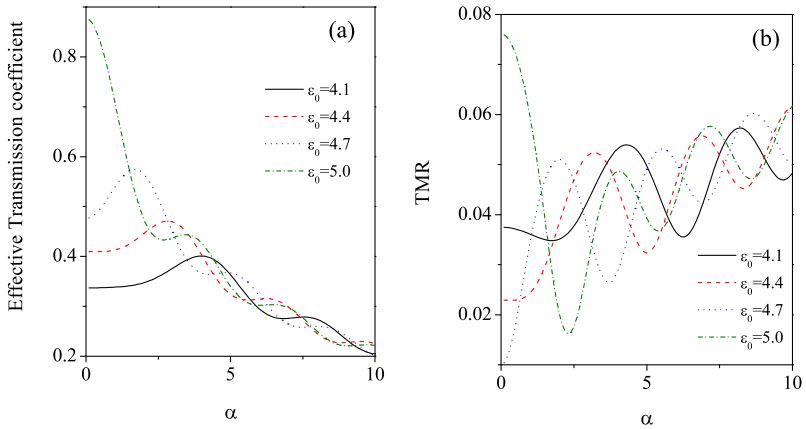


FIG. 14: (Color online) The α dependence of the ETC (a) and the TMR (b) for different energy levels in the central spacer. The parameters are taken as $\omega_0 = 0.3$, $P = 0.6$, $\eta = 10$, and $E_f = 5$, where $\theta = \pi/3$ for (a).

The α dependence of the ETC and the TMR for different ε_0 is shown in Figs. 14(a) and (b). One may observe that

(i) the ETC oscillates damply with increasing α, and a larger α may suppress the transmission; (ii) the TMR oscillates with increasing α; (iii) the peaks are sharper and more obvious when ε_0 closes to the main resonance and the photonic sidebands; (iv) when ε_0 leaves the main resonance energy to a lower value, the first resonant peak of the ETC and the TMR moves towards the direction of larger α's. These characters are the consequences of the photonic sidebands induced by the ac field. Here we should point out that the scattering mechanisms of electrons tunneling process assisted by phonon and by photon are fundamentally different. Interestingly enough, however, the features of photon-assisted and optical phonon-assisted tunneling current and conductance are similar, because both tunneling processes are assisted by sidebands induced by photons or optical phonons. In the conventional semiconductor tunnel diodes, the tunneling transitions are dominant by emission of phonon at low temperature (see Ref.[38]), while the present tunneling transitions are contributed by emission or absorption photon quantum. This photon-assisted tunneling in superconductor tunnel junctions was discussed in Ref.[39]. The resonant level is modulated not just by a displacement by emitting or absorbing photons, but is modulated in terms of a probability amplitude which is characterized by the square of the nth Bessel function $J_n(V_0/\omega_0)$ for each level to be displaced in energy by $n\omega_0$. These probability amplitudes contain the information about the quantum interference. The tunneling probability of electrons via these virtual energy levels may be modulated by these quantum interferences. In addition, the photon-assisted tunneling can be controlled by tuning an external ac field, but the phonon-assisted tunneling is primarily determined by the material. In the present case, the photon-assisted spin-dependent resonant tunneling is considered and the photon-assisted TMR is observed. This effect may be used to give a tunable TMR, which may be useful for future application. Recently, we have noted that a similar phonon-assisted tunneling through a molecular quantum dot was considered in Ref.[40].

V. SUMMARY

We have discussed the spin-dependent transport in a resonant tunneling structure with ferromagnetic multi-terminal under dc and ac fields by means of the nonequilibrium Green function technique. The general formulation of the time-dependent spintronic transport in this structure in the presence of ac and dc fields has been established, which might offer a fundamental basis for further discussions on the spin-dependent transport in such spintronic devices in an ac field.

First, we have considered the resonant system with two FM terminals in which the magnetizations of the leads are noncollinearly aligned under a dc bias voltage, and have found that for small η's where η characterizes the asymmetry of the relaxation times of the electrons with different spin in the central region, the TMR is negative, and whose absolute magnitude increases with increasing θ (the relative angle between the magnetizations of both leads); when η becomes larger, the TMR will be positive and increases with increasing θ. We have also investigated the TMR as a function of energy, the dc bias voltage and the gate voltage for different polarizations and energy levels of the central scattering region, respectively. The results are diverse, which manifest the effect of the resonant energy level on the TMR and the tunneling current, as discussed in detail in Sec.II.

Second, we have considered a three-terminal device under a dc bias, which is different from the standard three-terminal device discussed elsewhereRefs.[19, 20]. In the present device, each terminal is applied with a source bias, suggesting that there is net current flowing through every terminal. Regardless of the spin-flip scattering, the electrons in up-spin subbands in one terminal will be accepted by the up-spin subbands in another terminal. When the magnetizations of the first and second terminals are antiparallel, the change of θ which is the relative angle between the magnetizations of the first and third terminals may considerably change the current flowing out of the second terminal. It turns out that tuning θ the current can be remarkably enhanced, giving rise to the so-called magnetization configuration-induced enhancement of the current or the current ratio $\kappa_{2,P(AP)}(\theta)$. It has been found that the $TMR_3(\theta)$, which is defined in this case by the current change ratio when the configuration of the magnetizations of the first and second terminals is turned from parallel to antiparallel, decreases with increasing θ.

Third, as an application of our general formulation we have investigated the time-dependent spintronic transport in a system with two terminals under an ac field. We have uncovered that, when a very small dc bias is applied to the two terminals but an ac field is applied to the central scattering region, the photonic sidebands are formed in the central region. When the sidebands meet with the Fermi energy of the terminals, the photon-assisted tunneling will occur. It manifests as the resonant peaks in the ETC versus ε_0. The TMR exhibits many resonant peaks at the main resonant level and the photonic sidebands. It has been found that the asymmetric factor η may lead to additional peaks besides the photon-assisted resonant peaks. We would like to mention that the present study might open a way to control the spin-dependent transport in a spintronic device by applying a time-dependent electrical field.

Acknowledgments

This work is supported in part by the National Science Foundation of China (Grant Nos. 90103023, 10104015, 10247002).

[] *Corresponding author. Email address: gsu@gscas.ac.cn.

[1] M. N. Baibich, J. M. Broto, A. Fert, F. Nguyen Van Dau, P. Etienne, G. Creuzet, A. Friederch, and J. Chazelas, Phys. Rev. Lett. **61**, 2472 (1988).

[2] R. Meservey and P.M. Tedrow, Phys. Rep. **238**, 173 (1994); M. A. M. Gijs and G. E. W. Bauer, Adv. Phys. **46**, 285 (1997); J. S. Moodera, J. Nassar and G. Mathon, Annu. Rev. Mater. Sci. **29**, 381 (1999); S. A. Wolf et al, Science **294,** 1488 (2001); and references therein.

[3] S. S. Parkin, N. More, and K. P. Roche, Phys. Rev. Lett. **64**, 2304 (1990).

[4] M. D. Stiles, Phys. Rev. B **48**, 7238 (1993).

[5] P. Bruno, Phys. Rev. B **52**, 411 (1995).

[6] F. J. Himpsel, J. Phys.: Condens. Matter. **11**, 9483 (1999).

[7] J. C. Slonczewski, Phys. Rev. B **39**, 6995 (1989).

[8] L. Sheng, Y. Chen, H. Y. Teng, and C. S. Ting, Phys. Rev. B **59**, 480 (1999).

[9] K. Ono, H. Shimada, and Y. Ootuka, J. Phys. Soc. Jpn. **66**,1261 (1997).

[10] J. Barnaś and A. Fert, Phys. Rev. Lett. **80**, 1058 (1998).

[11] J. Barnaś, J. Martinek, G. Michalek, B. R. Bulka, and A. Fert, Phys. Rev. B **62**, 12363 (2000); B. R. Bulka, J. Martinek, G. Michalek, and J. Barnaś, Phys. Rev. B **60**, 12246 (1999).

[12] S. Takahashi, and S. Maekawa, Phys. Rev. Lett. **80**, 1758 (1998); H. Imamura, S. Takahashi, and S. Maekawa, Phys. Rev. B **59**, 6017 (1999).

[13] X. H. Wang, and A. Brataas, Phys. Rev. Lett. **83**, 5138 (1999).

[14] J. Iñarrea, and G. Platero, Europhys. Lett., **34**, 43 (1996); A. P. Jauho, cond-mat/9711141.

[15] M. Johnson, Science **260**, 320 (1993); G. A. Prinz, Phys. Tod. April (1995) 58.

[16] A. Fert and S. F. Lee, Phys. Rev. B **53**, 6554 (1996).

[17] S. Hershfield, and Hui Lin Zhao, Phys. Rev. B **56**, 3296 (1997).

[18] M. Büttiker, IBM. J. Res. Develop. **32,** 317 (1988); S. Datta, *Electronic Transport in Mesoscopic Systems* (Cambridge University Press, 1995).

[19] A. Brataas, Yu. V. Nazarov, and Gerrit E. W. Bauer, Phys. Rev. Lett. **84,** 2481 (2000).

[20] A. Brataas, Yu. V. Nazarov, and Gerrit E. W. Bauer, Eur. Phys. J. B **22,** 99 (2001).

[21] M. Johnson, J. Byers, Phys, Rev. B **67**, 125112 (2003).

[22] F. J. Jedema, A. T. Filip, and B. J. van Wees, Nature **410,** 345 (2001).

[23] F. J. Jedema, M. S. Nijboer, A. T. Filip, and B. J. van Wees, cond-mat/0111092.

[24] N. S. Wingreen, K. W. Jacobsen, and J. W. Wilkins, Phys. Rev. B **40**, 11834 (1989).

[25] A. M. Bratkovsky, Phys. Rev. B **56**, 2344 (1997).

[26] W. Rudziński, and J. Barnaś, Phys. Rev. B **64**, 085318 (2001).

[27] The spin accumulation can be estimated by calculating the difference of the diagonal elements of the matrix of the lesser Green function in spin space, say, $M = \langle N_{d\uparrow}\rangle - \langle N_{d\downarrow}\rangle = -i\{[G_d^<(t,t)]_{11} - [G_d^<(t,t)]_{22}\}$, where the definitions of the lesser Green function matrix $G_d^<(t,t)$ can be found in the following context. We shall study it elsewhere.

[28] Baigeng Wang, Jian Wang, and Hong Guo, Phys. Rev. Lett. **82,** 398 (1999).

[29] J. Q. You, Chi-Hang Lam, and H. Z. Zheng, Phys. Rev. B **62**, 1978 (2000).

[30] M. P. Anantram, and S. Datta, Phys. Rev. B **51,** 7632 (1995);

[31] A. P. Jauho, N. S. Wingreen, and Y. Meir, Phys. Rev. B **50,** 5528 (1994); H. Haug and A. -P. Jauho, *Quantum Kinetics in Transport and Optics of Semiconductors* (Springer-Verlag, Berlin, 1998).

[32] Zhen-Gang Zhu, Gang Su, Qing-Rong Zheng, and Biao Jin, Phys. Lett. A **300**, 658 (2002); Zhen-Gang Zhu, Gang Su, Biao Jin, and Qing-Rong Zheng, Phys. Lett. A **306,** 249 (2003).

[33] Tai-Kai Ng, Phys. Rev. Lett. **76**, 487 (1996).

[34] G. A. Prinz, Science **282**, 1660 (1998).

[35] Baigeng Wang, Jian Wang, and Hong Guo, J. Phys. Soc. Jpn. **70**, 2645 (2001).

[36] J. S. Moodera, J. Nowak, and R. J. M. van de Veerdonk, Phys. Rev. Lett. **80**, 2941 (1998).

[37] M. Johnson, and R. H. Silsbee, Phys. Rev. B **35**, 4959 (1987).

[38] R. A. Logan, and A. G. Chynoweth, Phys. Rev. **131**, 89 (1963).

[39] J. R. Tucker and M. J. Feldman, Rev. Mod. Phys. **57**, 1055 (1985).

[40] A. S. Alexandrov, and A. M. Bratkovsky, Phys. Rev. B **67**, 235312 (2003).